

A GEOPHYSICAL STUDY OF MICROEARTHQUAKE ACTIVITY
NEAR BOWMAN, SOUTH CAROLINA

A THESIS

Presented to

The Faculty of the Division of Graduate
Studies and Research

by

John H. McKee

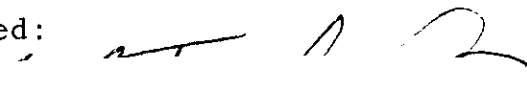
In Partial Fulfillment


of the Requirements for the Degree
Master of Science in Geophysical Sciences

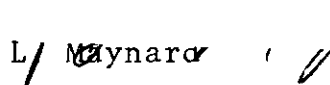
Georgia Institute of Technology

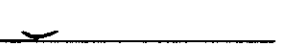
September, 1973

A GEOPHYSICAL STUDY OF MICROEARTHQUAKE ACTIVITY
NEAR BOWMAN, SOUTH CAROLINA

Approved: 


Dr. L. T. Long, Chairman


Dr. G. L. Maynard


Dr. R. P. Lowell

Date approved by Chairman: 9/7/73

ACKNOWLEDGMENTS

This thesis study was performed under the direction of Dr. L. T. Long, Associate Professor of Geophysics at Georgia Institute of Technology. The writer is indebted to Dr. Long who suggested this study, expedited the field operations and provided guidance throughout this work, particularly in the analysis of the data and the editing of the manuscript. Deep appreciation is also extended to Dr. G. L. Maynard and Dr. R. Lowell, the other members of the thesis committee who provided many helpful suggestions for editing the manuscript.

Gratitude is due Dr. Gilbert Bollinger of Virginia Polytechnical Institute who loaned two portable seismic systems which were critical to this work. Thanks go also to Dr. Norman K. Olson, State Geologist for South Carolina, and Dr. Art Tarr of NOAA who provided data used in this thesis. The writer is especially indebted to fellow students who worked long hours recording data and repairing equipment. These men are Nick Faust, Edward Denman, and Larry Brown, who were students of Geophysical Sciences at Georgia Institute of Technology, and David Weisenhorn, who was a student of Electrical Engineering at Georgia Institute of Technology.

During my tenure as a graduate student at Georgia Institute of Technology, I was awarded a research assistantship

supported by the National Science Foundation (Grant Number GA 31962) and was also employed part-time by the School of Geophysical Sciences. The experience I gained during my employments enhanced my knowledge of geophysics and contributed to work on this thesis.

TABLE OF CONTENTS

	Page
ACKNOWLEDGMENTS.	ii
LIST OF TABLES	v
LIST OF FIGURES.	vi
SUMMARY.	viii
CHAPTER	
I. INTRODUCTION.	1
II. GEOLOGIC SETTING AND VELOCITY MODEL	5
III. MICROEARTHQUAKE RECONNAISSANCE.	11
IV. GRAVITY DATA.	26
V. MAGNETIC DATA	36
VI. DISCUSSIONS AND CONCLUSIONS	38
VII. RECOMMENDATIONS	43
APPENDIX	
I. ANALYSIS OF SEISMIC DATA.	45
II. ANALYSIS OF GRAVITY AND MAGNETIC DATA	54
BIBLIOGRAPHY	64

LIST OF TABLES

Table	Page
1. List of Felt Earthquakes Near Bowman.	12
2. List of Microearthquakes Near Bowman Between August, 1972, and July, 1973.	13
3. List of Bowman Microearthquakes Recorded by Arrays.	21

LIST OF FIGURES

Figure		Page
1.	Seismic Map for South Carolina.	2
2.	Geologic Cross Section for the Bowman Area. . .	6
3.	Carn Farm Refraction Survey Data.	8
4.	Velocity Structure and Travel Time Curves . . .	10
5.	Records of the 1972 August 8, and 1973 December 16, Microearthquakes.	14
6.	Recording Station Locations and Epicenter of the 1973 December 16, Microearthquakes.	15
7.	Records of the 1973 March 22, 06h42m, Microearthquakes.	17
8.	Recording Station Locations and Epicenters of the 1973 March 22, Microearthquakes	18
9.	Records of the 1973 March 22, 14h42m, Microearthquake	20
10.	Digitized and Filtered Trace of the Carn Farm Array Data.	23
11.	Carn Farm Array Configuration	24
12.	Regional Simple Bouguer Anomaly Map	27
13.	Small Scale Simple Bouguer Anomaly Map.	29
14.	Comparison of Observed Profiles with Basement Structure Model Profiles.	30
15.	Gravity Profile of Detailed Line and Fault Models.	32
16.	Detailed Line Profiles with Various Bouguer Reduction Densities	33
17.	Regional Aeromagnetic Anomaly Map	37

Figure	Page
18. Distribution of Coastal Plain Microearthquakes from March to July, 1973.	41
19. Acceleration Response Curves and Particle Velocity Curves	46

SUMMARY

South Carolina earthquakes can be interpreted as forming a NW-SE trending zone of seismic activity that extends from Charleston to the Appalachians. Prior to the occurrence in 1971, and 1972, of a sequence of four intensity III or more earthquakes near Bowman, South Carolina, the area between Columbia and Charleston represented a significant apparent gap in this proposed zone.

From August, 1972, to March, 1973, microearthquake reconnaissance surveys near Bowman recorded six microearthquakes. Three were located to within ± 3 km. These microearthquake epicenters were insufficient to define a specific fault plane through the Bowman area. However, other recent microearthquakes near Lexington, South Carolina, and in the Charleston-Summerville area lend support to a hypothesized zone of seismic activity which passes through Bowman.

Three hundred and forty-four new points of gravity data in the vicinity of Bowman suggest that a nearly linear high density basement structure trending NE-SW underlies much of the Bowman microearthquake epicentral area. Magnetic data indicates that the structure also exhibits a higher magnetic susceptibility than the surrounding basement material. Using data from a geophone array which recorded

one of the Bowman microearthquakes, a basement velocity of 6.3 km/sec \pm 0.7 km/sec was computed for the epicentral area. The high values for density, velocity and susceptibility of the basement structure imply that it is possibly diabase.

Irregularities in the gravity contour lines defining the linear anomaly appear to strike NW-SE. Analysis of a line of dense gravity data indicates that a steep 1.3 mgal gravity anomaly may be responsible for the NW-SE trending perturbations. Theoretical gravity profiles generated by two dimensional fault models closely approximate the steep anomaly observed in the profile of the detailed gravity line provided the modeled fault is placed at a depth of 0.32 km or less.

CHAPTER I

INTRODUCTION

The seismic history of South Carolina is dominated by the Charleston earthquake of August 31, 1886, its fore-shocks and its aftershocks. The 1886 August 31, event initiated a period of increased seismic activity that lasted for approximately thirty years (Bollinger, 1972). This earthquake was felt over an area of approximately 2,000,000 square miles, including the undersea area, and it was felt with an intensity II (Rossi-Forel) as far away as New York and Bermuda. Savannah and Columbia, two cities approximately 90 miles from Charleston, experienced intensities of VIII and VIII to IX (Rossi-Forel), respectively (Dutton, 1889). In both cities, many chimneys were damaged, and some buildings suffered minor structural damage. In Charleston, the earthquake caused extensive damage and was rated as an intensity X on the Rossi-Forel scale.

Between 1754 and 1971, a total of 438 earthquakes have been reported as occurring in South Carolina (Bollinger, 1972). Of these, 402 have been located in the Charleston-Summerville area. Figure 1 shows the distribution of earthquakes in South Carolina through 1971. In the neighboring states of Alabama, North Carolina and Tennessee,

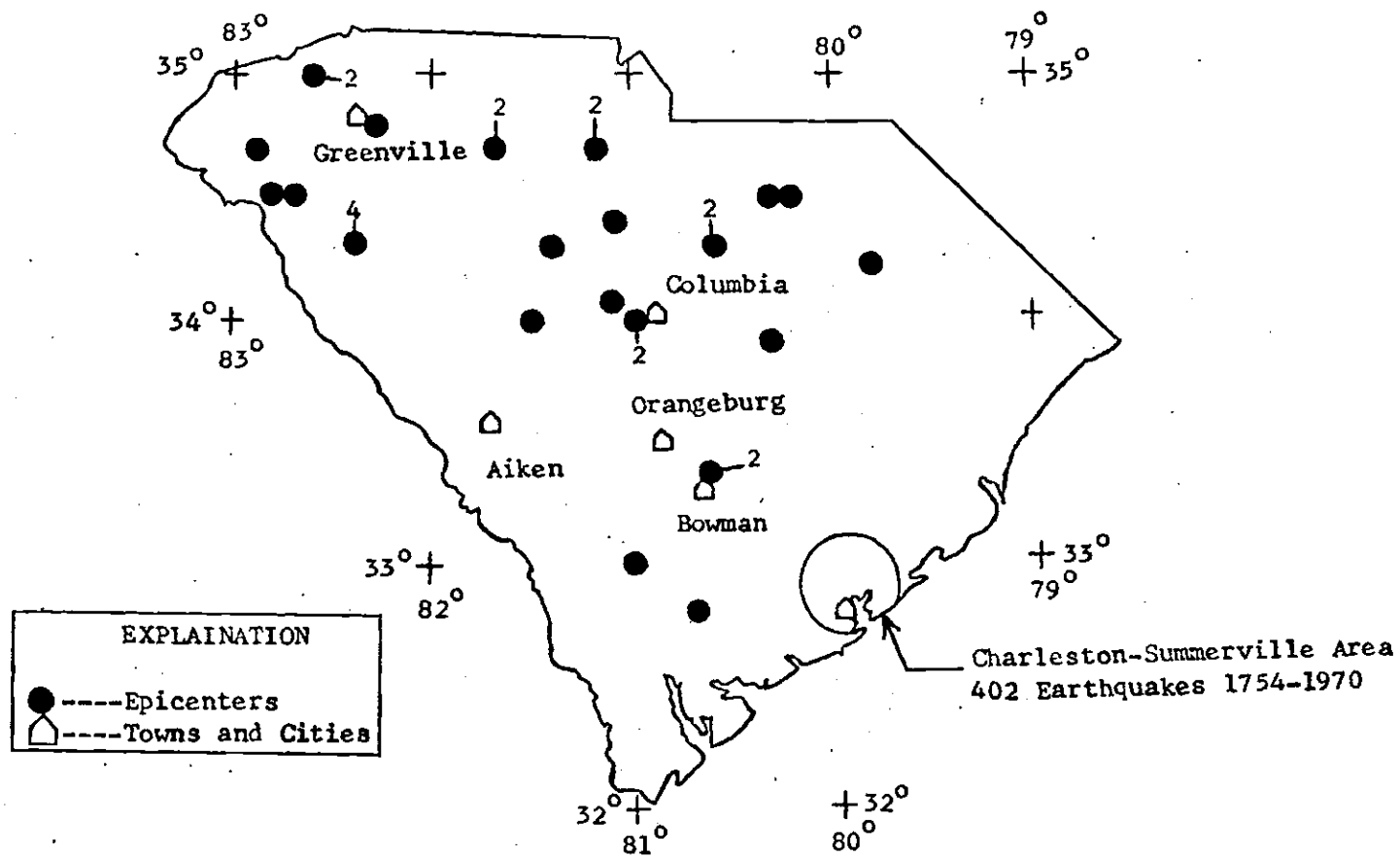


Figure 1. Seismicity Map for South Carolina (after Bollinger, 1972).
Numbers Indicate Multiple Events.

epicenters generally trend NE-SW, paralleling the Appalachian structure. Multiple zones of seismic activity may parallel these zones in South Carolina. Many, for example Taber (1914), believe that the Charleston event of August, 1886, lies in a NE-SW trending zone near the coast.

Bollinger (1972) has interpreted the South Carolina events as forming a NW-SE trending zone of seismic activity that extends from Charleston to the Appalachians. This proposed belt of earthquake epicenters is perpendicular to the regional structure, but it parallels the numerous NW-SE oriented Mesozoic diabase dikes which are found in Alabama and South Carolina (Bollinger, 1972).

Prior to 1971, few earthquakes had been reported as occurring in central South Carolina. The region between Columbia and Charleston represented a significant apparent gap in the proposed NW-SE trending zone of seismic activity. Prior to May 19, 1971, Bowman, South Carolina, which is roughly midway between Columbia and Charleston, had no record of seismic activity within a radius of 50 km (Long, 1972). At 12:53 GMT on May 19, 1971, a maximum intensity IV (Modified Mercalli) earthquake occurred near Bowman. Within a period of eighteen months three additional events occurred. The largest and most recent event in the sequence was felt with an intensity V on February 3, 1972. Two aftershocks were felt with an intensity III on February 7, 1972. Several additional microearthquakes have subsequently been recorded

by portable smoked paper seismometers and interpreted as occurring within five kilometers of Bowman. These events are located approximately 60 kilometers northwest of the presumed epicenters of the August, 1886, Charleston earthquake.

The February 3, 1972, earthquake was the largest event which has been recorded in the Southeast since the installation of seismic station ATL in 1963. It was felt with an intensity of II to V (Modified Mercalli) over an area of 26,000 square miles, and Long (1972) computed its magnitude (M_L) to be 4.7. If it occurred along a previously active fault zone, the cumulative displacement could be large enough to be detected by geophysical survey methods. The continuing intermittent microearthquake activity also suggested that seismic data might provide enough epicenter locations to define the fault plane.

The purpose of this thesis study has been to investigate, using geophysical survey techniques, the nature and cause of the microearthquake activity near Bowman, South Carolina. Recently acquired microearthquake reconnaissance data and gravity data have been combined and correlated with existing geologic and seismic data. An attempt has been made to relate the Bowman microearthquake activity to the NW-SE trending zone of seismic activity hypothesized by Bollinger (1972) to extend across South Carolina from Charleston to the Appalachians.

CHAPTER II

GEOLOGIC SETTING AND VELOCITY MODEL

Bowman is located in Orangeburg County. Geologically, Orangeburg County is classed as the Lower Coastal Plain, and topographically it is essentially flat and featureless. Virtually all of the area's relief is due to sinkholes and the numerous NW-SE trending creeks and swamps. Elevations in the epicentral area vary from approximately 34 meters to almost 52 meters.

Figure 2 shows the distribution of major stratigraphic units present in the area of interest. According to Pooser (1965) the epicentral region is underlain by the Duplin Formation, the Santee Limestone and the Black Mingo Formation. The Black Mingo Formation underlies an extensive area, and it consists of quartzose sand, thin layers of silty clay and dark gray unctuous clay with small particles of Fuller's earth and pyrite. This layer ranges in thickness from 9 meters to as much as 38 meters. Much of the Black Mingo Formation was deposited in estuaries and littoral environments.

The Santee Limestone is a calcilutite to calcirudite that varies in color from creamy white to yellow. It is consolidated but not well indurated and is very fossiliferous.

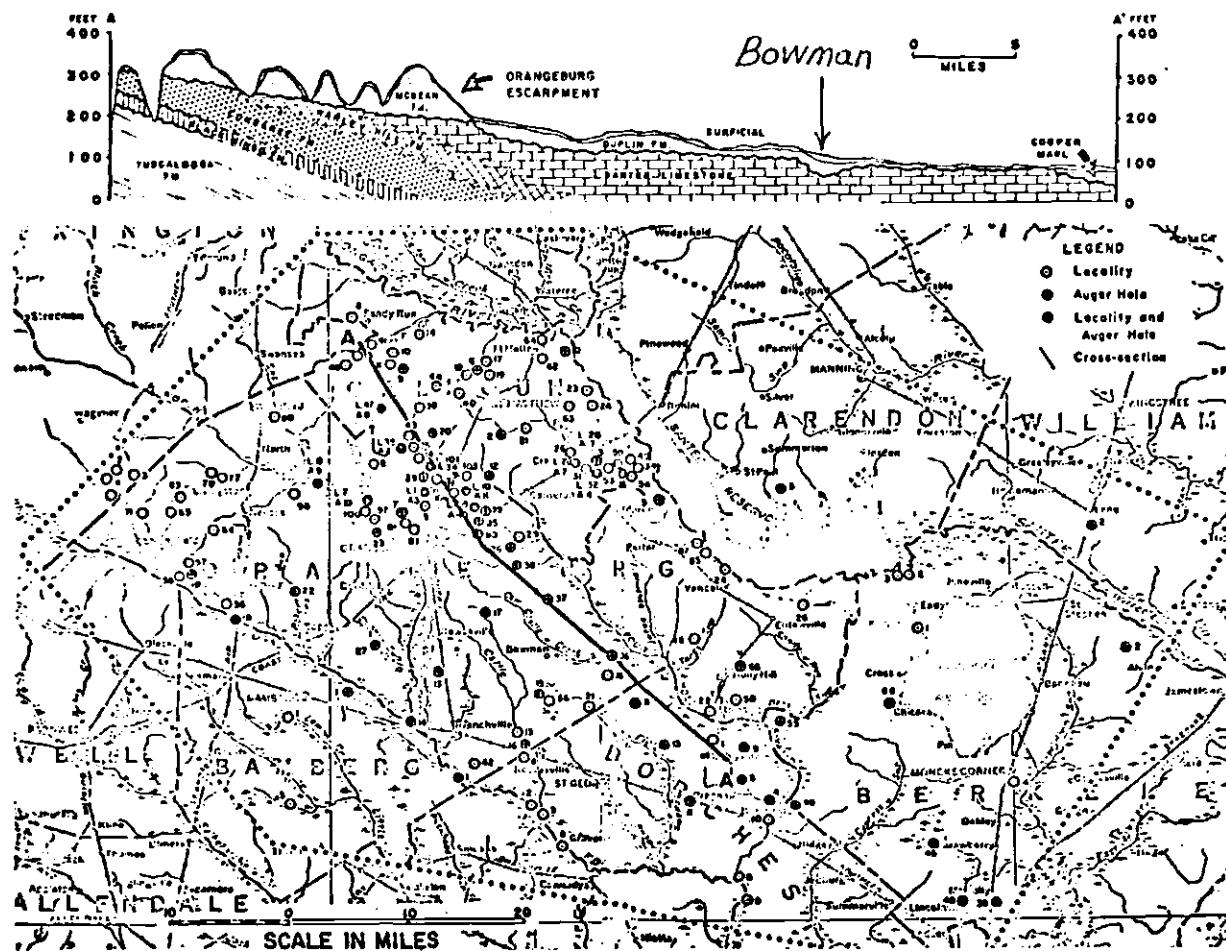


Figure 2. Geologic Cross Section A-A' Showing the Disposition of the Major Stratigraphic Units in the Bowman Area (after Pooser, 1965).

Near Bowman, it is overlain by a thin veneer of the Duplin Formation. The Duplin Formation is difficult to distinguish from the overlying surficial material. It is composed primarily of noncalcareous and calcareous quartzose sands with numerous shells (Pooser, 1965).

A refraction survey at Carn's Farm (see Figure 9) was conducted in an attempt to determine near surface velocities. The equipment used consisted of a portable tape recorder, amplifiers and 15 Hz exploration geophones. One geophone was used as a "shot break" and was moved progressively closer to the recording geophone beginning at a distance of 110 meters. A total of six "shots" were recorded. The energy source was a heavy object dropped from a height of nearly 2 meters. A first arrival corresponding to the direct P wave and a Rayleigh wave arrival were observed on each of the six records. Analysis of the data yielded apparent velocities of $0.81 \text{ km/sec} \pm 0.08 \text{ km/sec}$ and $0.24 \text{ km/sec} \pm 0.02 \text{ km/sec}$ for the P and Rayleigh waves respectively (Figure 3). Using the equations of White (1965, p 102), the velocity of the S wave was computed to be $0.25 \text{ km/sec} \pm 0.03 \text{ km/sec}$. The uncertainty in these numbers is due to uncertainty in interpreting the phase arrival times; however, these velocities are typical of sandy soils and unconsolidated formations such as the Duplin Formation. The velocities are representative of the surface layers (approximately 15 meters) only.

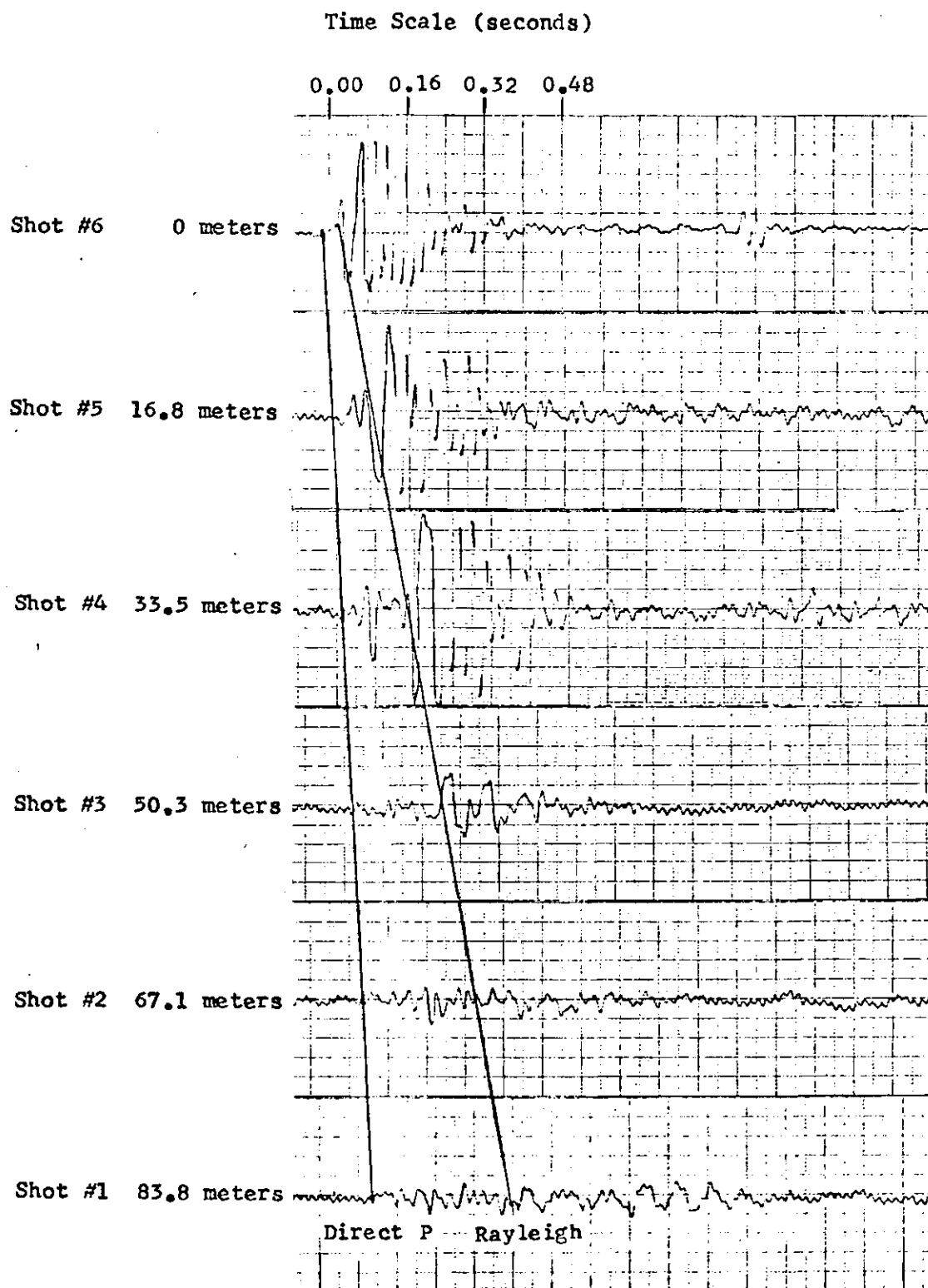


Figure 3. Carn Farm Refraction Survey Data.

Seismic refraction work by Woollard et al. (1957) was used to define the deeper velocity structure for the Bowman area. Data from refraction lines located north and west of Bowman in Orangeburg County and one southeast of Bowman in Dorchester County were used to interpolate the velocities and the depth to basement in the epicentral region. Both the depth to basement and the velocities of the surface layer appear to increase linearly to the southeast. The interpolated values for the depth to basement and the surface layer velocity are 460 meters and 2.4 km/sec respectively. The basement velocities show more variation and a linear interpolation is not justified. However, on the basis of the surrounding refraction data, 6.1 km/sec was considered for a first estimate for the basement velocity. Figure 4 shows the velocity structure and travel time curves computed for basement velocities of 6.9 km/sec. Standard time-distance relations for the two layer case were used in computing these curves (Dobrin, 1960).

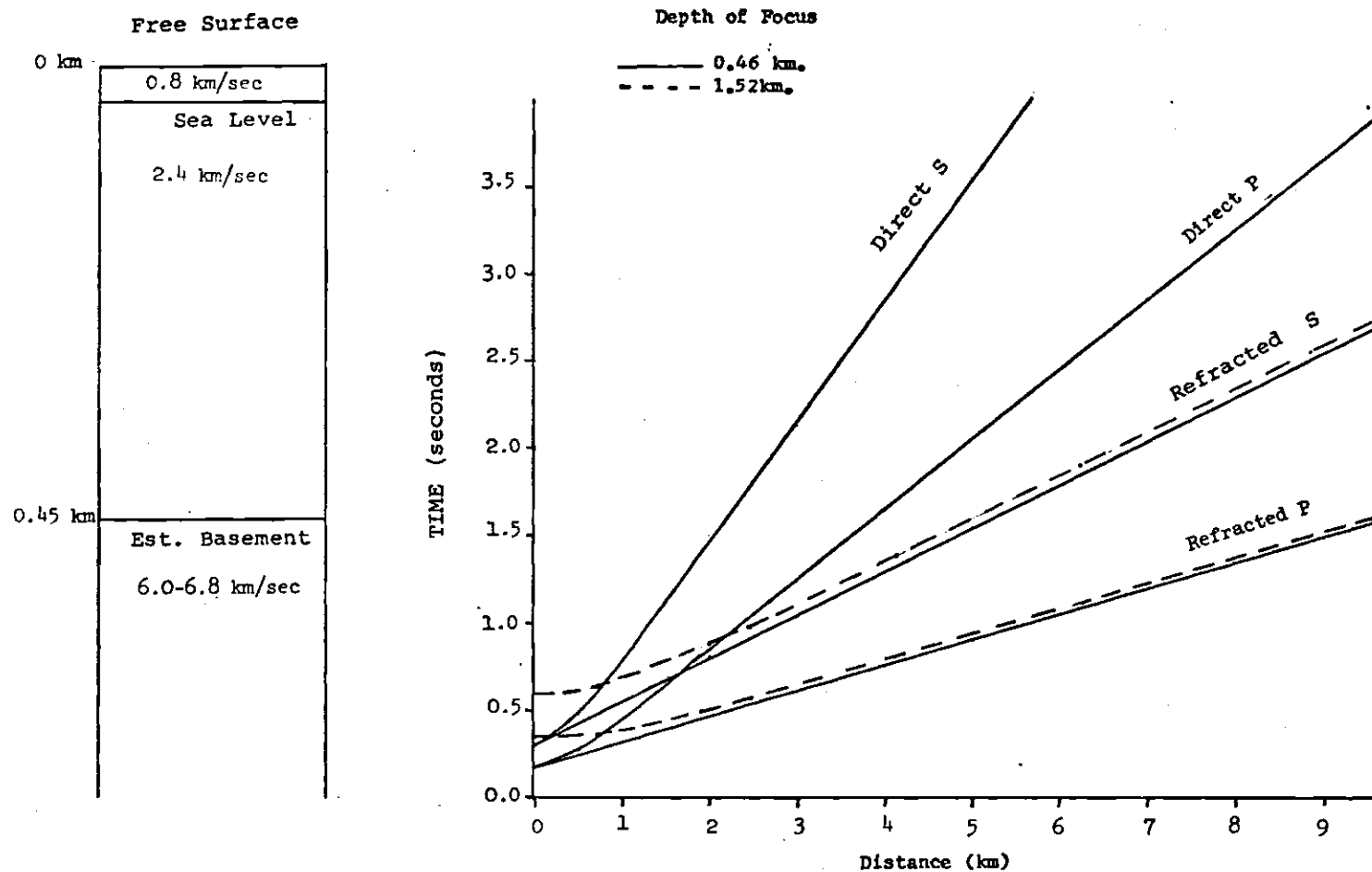


Figure 4. Velocity Structure and Travel Time Curves for a Basement Velocity of 6.9 km/sec. Travel Time Curves are Plotted for Focal Depths of 0.46 km and 1.52 km.

CHAPTER III

MICROEARTHQUAKE RECONNAISSANCE

Long (1972) computed the location of the epicenter of the 1972 February 3, event to be approximately 14 km north-east of Bowman. Subsequent to this, four microearthquake reconnaissance surveys were conducted in the vicinity of Bowman, resulting in approximately 20 days of noise-free recordings by three or more instruments. Additional data were obtained from a single smoked paper seismograph which recorded in Bowman for a ten week period from May through July, 1973.

Table 1 lists felt events which were recorded by station ATL and were located in the Bowman area. The times and locations of microearthquakes which were located in Bowman or immediately adjacent areas of the proposed NW-SE trending belt of seismic activity are given in Table 2. The list includes events from August 8, 1972, through July 1, 1973.

On August 8, 1972, a single portable seismograph located at Meyers Farm recorded a microearthquake (Figure 5). Analysis of the (S-P) time indicated the distance to the epicenter of the event to be $4.5 \text{ km} \pm 0.5 \text{ km}$. In December, 1972, a four station rectangular array was established with Meyers Farm as the southern corner of the rectangle (Figure 6).

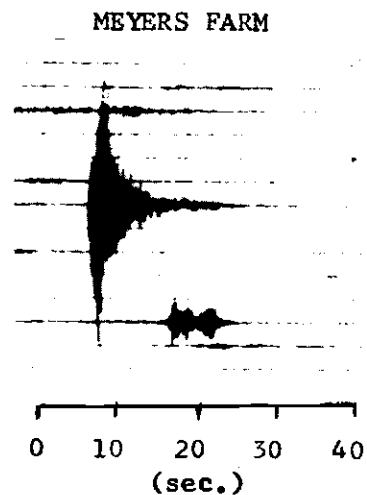
Table 1. List of Felt Earthquakes Located near Bowman, South Carolina
and Recorded by ATL and other Stations

Date - Time (GMT)	Maximum Intensity	M _L (from ATL records)	ATL Amplitude	Latitude	Longitude	Remarks
1971 May 19, 12h52m60s	IV	4.3	20.8	33.3°N	-80.6°W	NOAA
1971 July 31, 20h16m52s	III	4.3	20.	33.4°N	-80.7°W	NOAA
1971 August 11, 03h50m	I-II	3.9	9.26	--	--	ATL and BLA records indicate Orangeburg area
1972 February 3, 23h11m08s	V	4.7	69.3	33.46°N 33.476°N	-80.58°W -80.434°W	Long (1973) NOAA
1972 February 7, 02h46m	III	3.1	3.1	33°.46°N	-80.58°W	Long (1973)
1972 February 7, 02h53m	III	2.0	2.0	33°.46°N	-80.58°W	Long (1973)

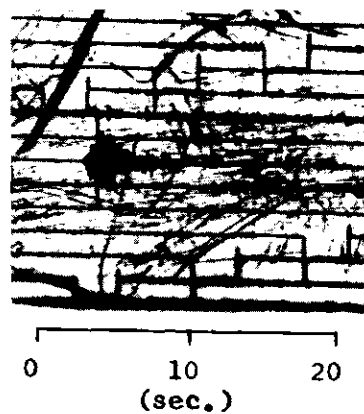
Table 2. List of Events which Occurred Between August 8, 1972 and July 1, 1973 and were Located in Bowman or Adjacent Areas of the Proposed NW-SE Trending Zone of Seismic Activity

Date - Time (GMT)	Location	Remarks
1972 August 8, 08h00m	33°22.5'N-80°36.4'W+6km	recorded by one instrument near Bowman
1972 December 16, 06h52m	33°22.5'N-80°41.3'W+2km	recorded by three stations near Bowman
1973 March 22, 06h42m	33°28.5'N-80°43.0'W+3km	recorded by three stations near Bowman
1973 March 22, 14h42m	33°22.8'N-80°40.5'W+1km	recorded by four stations near Bowman
1973 March 25, 04h29m	33°04.2'N-80°06.9'N	NOAA--three detections
1973 March 27, 08h00m	Lexington, South Carolina	felt in Lexington
1973 March 27, 11h00m	Lexington, South Carolina	felt in Lexington
1973 April 1, 13h26m	33°02.4'N-80°08.9'W	NOAA--four detections
1973 April 1, 13h44m	33°02.2'N-80°07.0'W	NOAA--three detections
1973 April 1, 18h30m	33°00.7'N-80°09.0'W	NOAA--three detections
1973 April 18, 10h06m	33°02.4'N-80°16.7'W	NOAA--four detections
1973 May 4, 02h39m	33°02.0'N-80°10.2'W	NOAA--five detections
1973 May 27, 01h56m	33°20.8'N-80°40.6'W+5km	recorded by one instrument in Bowman
1973 June 9, 19h24m	32°55.7'N-80°09.8'W	NOAA--four detections also recorded in Bowman
1973 July 1, 08h20m	33°20.8'N-80°40.6'W	recorded in Bowman by one instrument, recorded at St. George, South Carolina (NOAA) by one station.

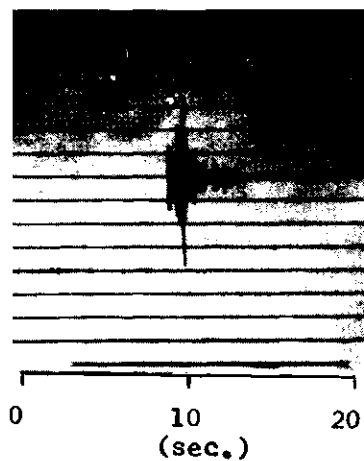
AUGUST 8, 1972
MICROEARTHQUAKE



DECEMBER 16, 1972
MICROEARTHQUAKE



WALNUT GROVE CHURCH



ISLAND CEMETERY

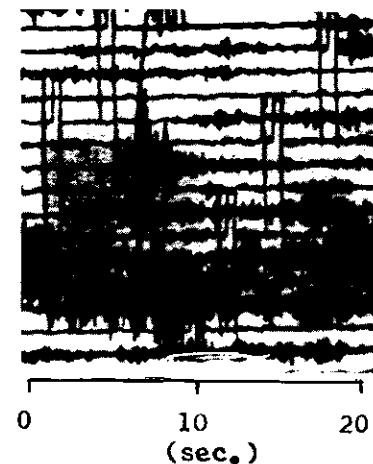


Figure 5. Photographs of the Smoked Paper Records of the 1972 August 8, and the 1972 December 16, Microearthquakes.

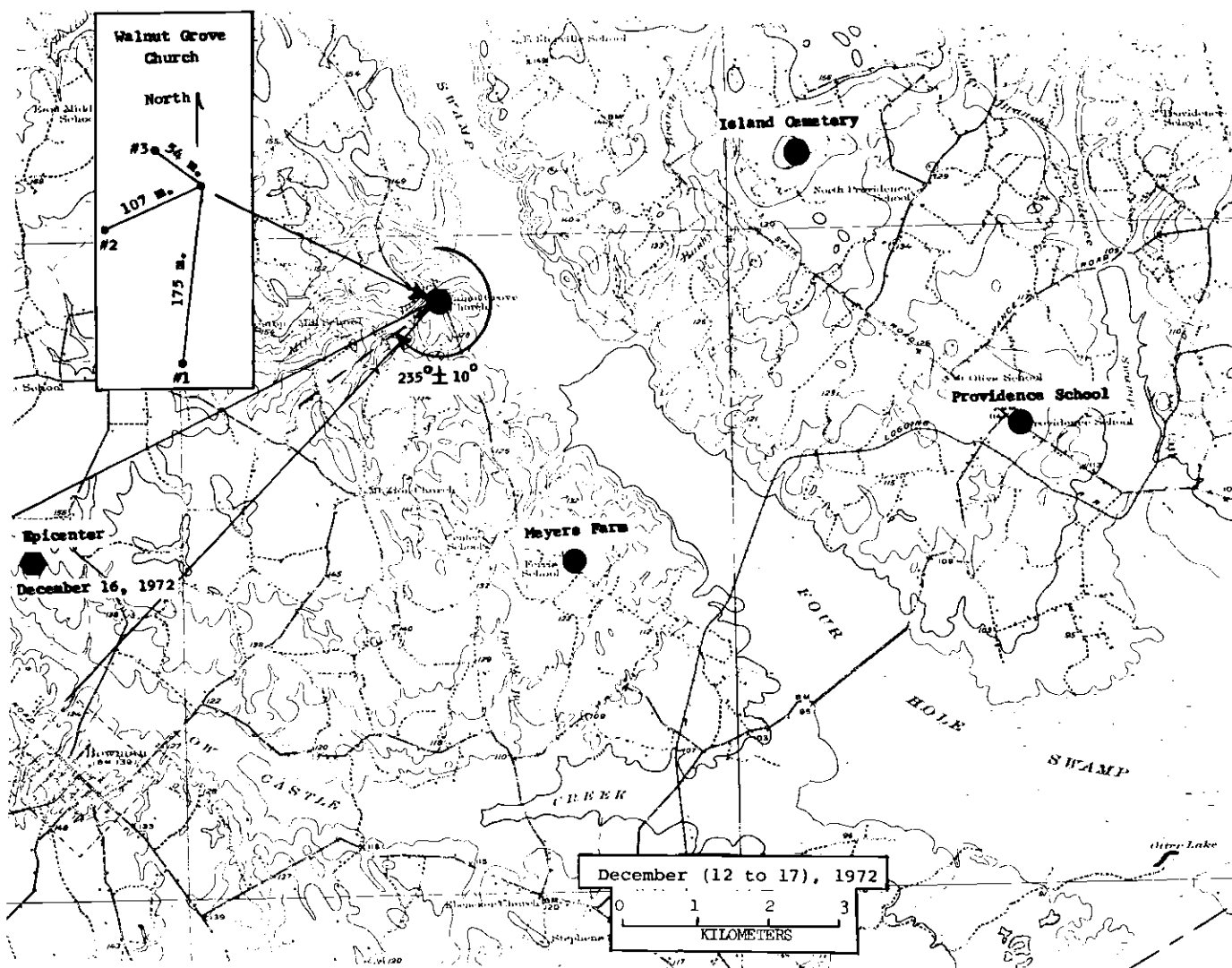


Figure 6. Recording Station Locations and Epicenter of the 1972 December 16, Microearthquake. The Array Insert is Centered at Walnut Grove Church. The Angle is the Azimuth from Walnut Grove Church to the Epicenter.

At Providence School the record of the event was hidden in background noise, but the smoked paper records of the other stations were sufficiently distinct for the identification of both P and S phases. A small geophone array at Walnut Grove Church recorded the event on magnetic tape and provided azimuthal control for the location of the epicenter. The azimuth from Walnut Grove Church to the epicenter of the event, measured clockwise from north, is $235^{\circ} \pm 10^{\circ}$ (precision based on 95% certainty).

Using a basement velocity of 6.1 km/sec, efforts to locate the epicenter for this event failed to achieve convergence (see Appendix I for epicenter location techniques) suggesting that a higher basement velocity was required. With an assumed basement velocity of 6.9 km/sec, the epicenter was located west of the array at $33^{\circ} 22.5'N-80^{\circ} 41.3'W$ with a precision of ± 2 km.

In March, 1973, two additional microearthquakes were recorded. The first event was recorded on 1973 March 22, 06h42m GMT by portable seismographs at Walnut Grove Church, Shiloh Church, Carn Farm and Bowman Cemetery (Figure 7). Three records were of good quality, but at Bowman Cemetery the event was barely recorded due to the low operating gain of the instrument. An interpretation of the (S-P) times of the event located the epicenter 18 km to the north of Bowman at $33^{\circ}28.5'N-80^{\circ}43.0'W$ with a precision of ± 3 km (Figure 8). This location was based on an assumed focal depth of 0.46 km

1973 MARCH 22, 06h42m GMT MICROEARTHQUAKE

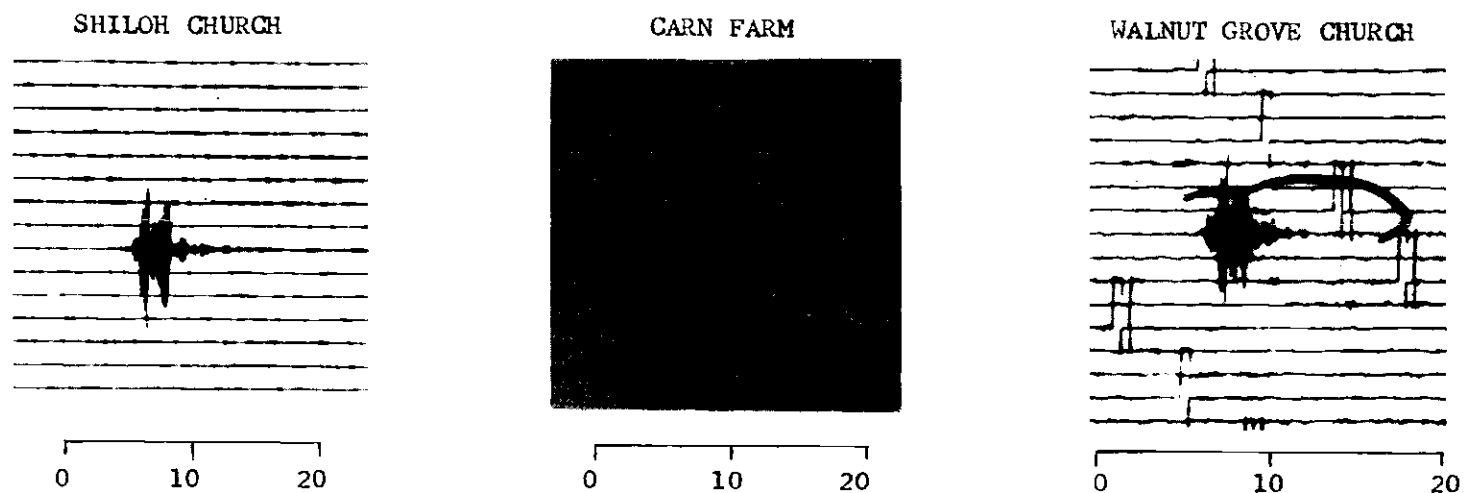


Figure 7. Photographs of the Smoked Paper Records of the 1973 March 22, 06h42m GMT Microearthquake.

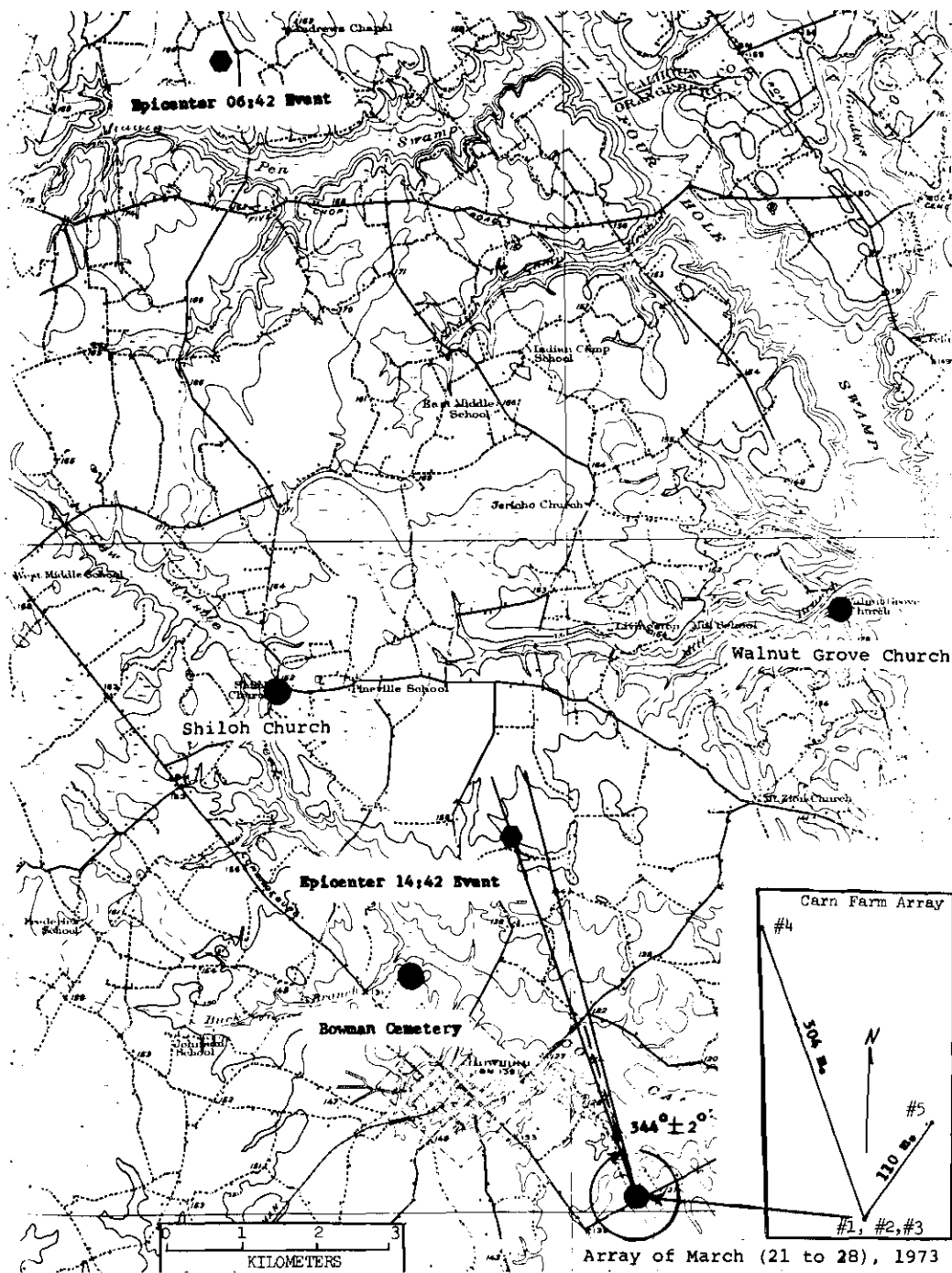


Figure 8. Recording Station Locations and Epicenters of the Two 1973 March 22, Microearthquakes. Array Insert is Centered at Carn Farm. The Angle is the Azimuth from Carn Farm to the Epicenter of the 14h42m GMT Event.

and a basement velocity of 6.9 km/sec.

The interpretation of the records of this event was made difficult by the low amplitude of the refracted P phase. The weak character of the refracted P phase could not be entirely attributable to recording distance. The 1972 December 16, event and the 1973 March 22, 06h42m GMT event were recorded at equivalent distances by seismographs at Island Cemetery and Walnut Grove Church respectively. The records of the events, however, showed refracted P phases of considerably different character. It is possible that differences in source mechanism, depth of focus or basement velocity structure could contribute to the variation. There were insufficient data to determine if there was any consistent azimuthal variation in the recorded character of the refracted P phase.

A second event was recorded at Walnut Grove Church, Shiloh Church and Bowman Cemetery by portable seismographs and at Carn Farm by both a portable seismograph and a small geophone array (Figure 9). The small array at Carn Farm recorded the microearthquake on magnetic tape. The event occurred on 1973 March 22, 14h42m GMT. Using a basement velocity of 6.9 km/sec and a focal depth of 0.6 km, the epicenter was located at $33^{\circ} 22.8'N-80^{\circ} 40.5'W$ with a precision of ± 1 km. Table 3 lists the origin times and epicenters of the three events recorded by arrays as well as the locations of the recording seismographs.

1973 MARCH 22, 14h42m GMT MICROEARTHQUAKE

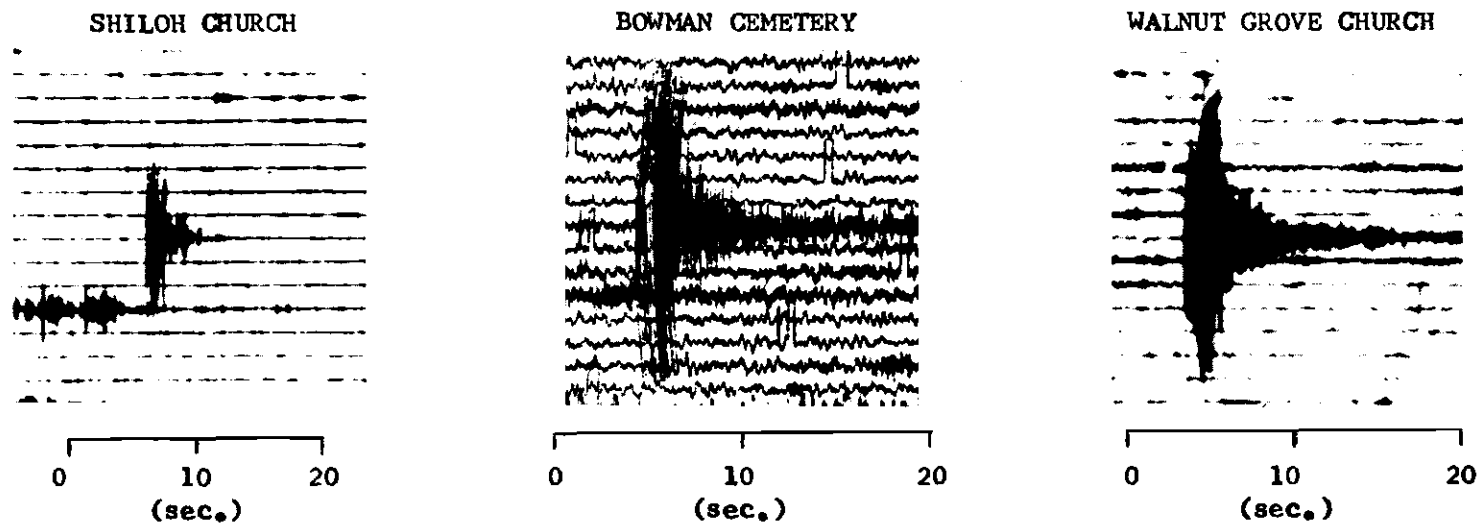


Figure 9. Photographs of the Smoked Paper Records of the 1973 March 22, 14h42m GMT Microearthquake.

Table 3. List of Microearthquakes
Recorded by Arrays

Event: December 16, 1972 Time: 06h52m GMT
 Location (Error-Grid): Lat. $33^{\circ} 22.5'$ Long. $80^{\circ} 41.3'$
 Location (Do-All): Lat. $33^{\circ} 22.57'$ Long. $80^{\circ} 41.26'$
 $T_0 = 0.02$ (sec)

<u>Recording Station</u>	<u>Latitude</u>	<u>Longitude</u>	<u>(S-P) (Seconds)</u>
Island Cemetery	33.426	80.573	1.39
Meyers Farm	33.375	80.606	0.94
Walnut Grove Church	33.408	80.626	0.86
Providence School*	33.392	80.540	--

Event: March 22, 1973 Time: 09h42m GMT
 Location (Error-Grid): Lat. $33^{\circ} 28.5'$ Long. $80^{\circ} 43.0'$
 Location (Do-All): Lat. $33^{\circ} 28.44'$ Long. $80^{\circ} 43.11'$
 $T_0 = 0.05$ (sec)

<u>Recording Station</u>	<u>Latitude</u>	<u>Longitude</u>	<u>(S-P) (Seconds)</u>
Walnut Grove Church	33.408	80.626	1.33
Carn Farm	33.335	80.657	1.88
Shiloh Church	33.399	80.709	1.04
Bowman Cemetery*	33.363	80.689	--

Event: March 22, 1973 Time: 14h42m GMT
 Location (Error-Grid): Lat. $33^{\circ} 22.8'$ Long. $80^{\circ} 40.5'$

<u>Recording Station</u>	<u>Latitude</u>	<u>Longitude</u>	<u>(S-P) (Seconds)</u>
Walnut Grove Church	33.408	80.626	0.69
Carn Farm	33.335	80.657	0.61
Shiloh Church	33.399	80.709	0.45
Bowman Cemetery*	33.363	80.689	--

*Records from these stations were of poor quality and, therefore, were not used in locating the epicenters.

The array at Carn Farm was a tripartite array with a three component geophone cluster at one corner. Five channels of data and one of time were recorded on a seven channel Honeywell tape unit. The data from the analog tape was filtered with a 100 Hz low pass filter, digitized and plotted (Figure 10).

The array size was measured to a precision of ± 2 meters (Figure 11). Arrival times across the array relative to channel 4 were:

$$\begin{array}{llll} \text{Ch 4} & 0.0 & \pm 0.005 \text{ sec} \\ \text{Ch 5} & 0.037 & \pm 0.005 \text{ sec} = t_1 \pm 0.005 \text{ sec} \\ \text{Ch 1,2,3} & 0.048 & \pm 0.005 \text{ sec} = t_2 \pm 0.005 \text{ sec} \end{array}$$

In the computations of the velocity and azimuth, the seismic wavefront was assumed to be a straight line as it crossed the array. If the wavefront makes an angle B with the line from Ch 4 to Ch 2, an analytic expression for the apparent velocity across the array is:

$$V_{ap} = \frac{D_1 \cos(B) - D_2 \cos(A-B)}{t_1} \quad (1)$$

$$V_{ap} = \frac{D_1 \cos(B)}{t_2} \quad (2)$$

These equations are satisfied when $B = 3.9^\circ$ and $V_{ap} = 6.3 \text{ km/sec}$. Since the errors in D_1 , D_2 and A are very small compared with the errors in t_1 and t_2 , the errors for ΔV and B can be computed by applying standard error analysis

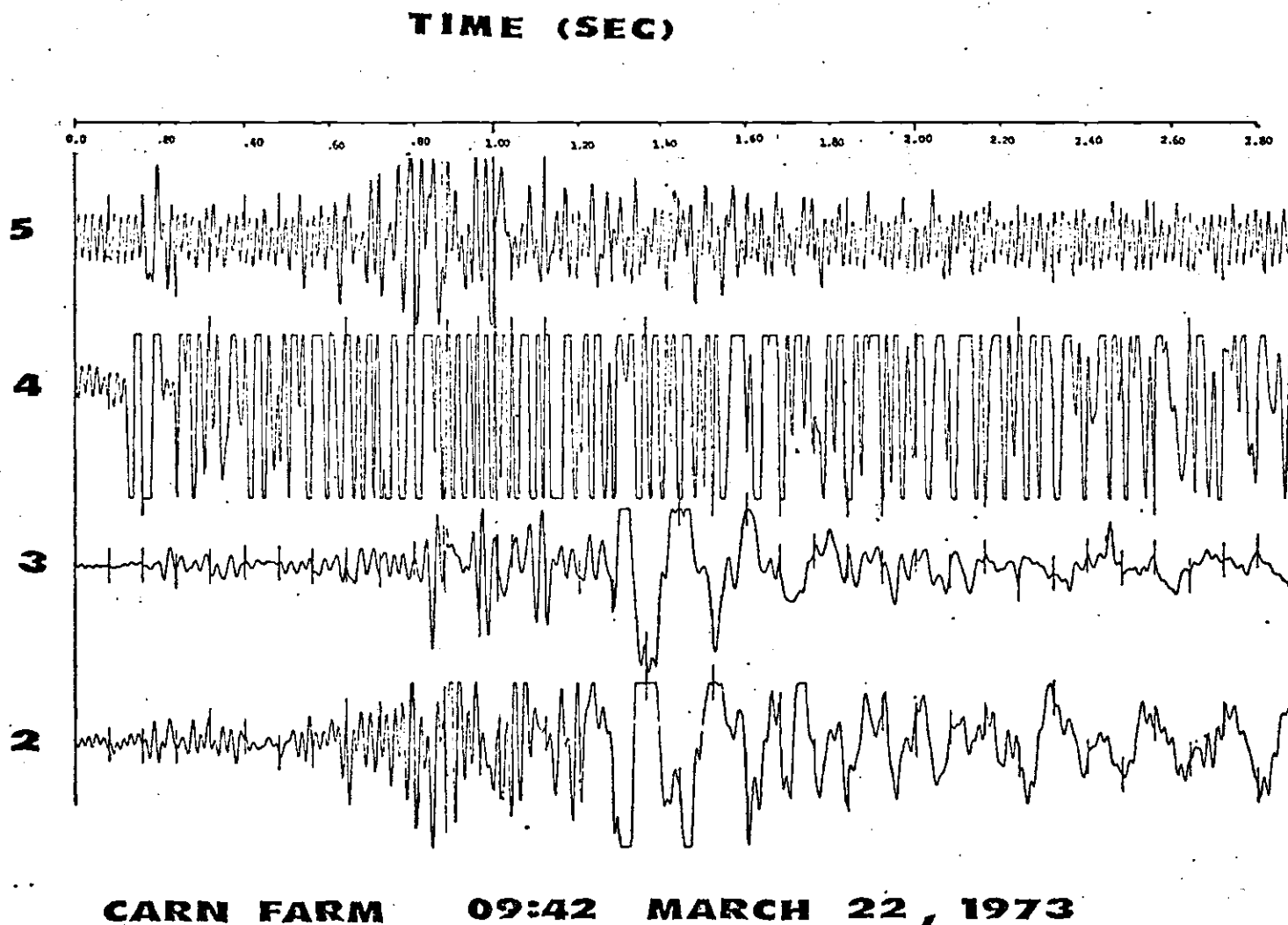


Figure 10. Digitized and Filtered Trace of the Carn Farm Array Recording of the 1973 March 22, 14h42m GMT Event.

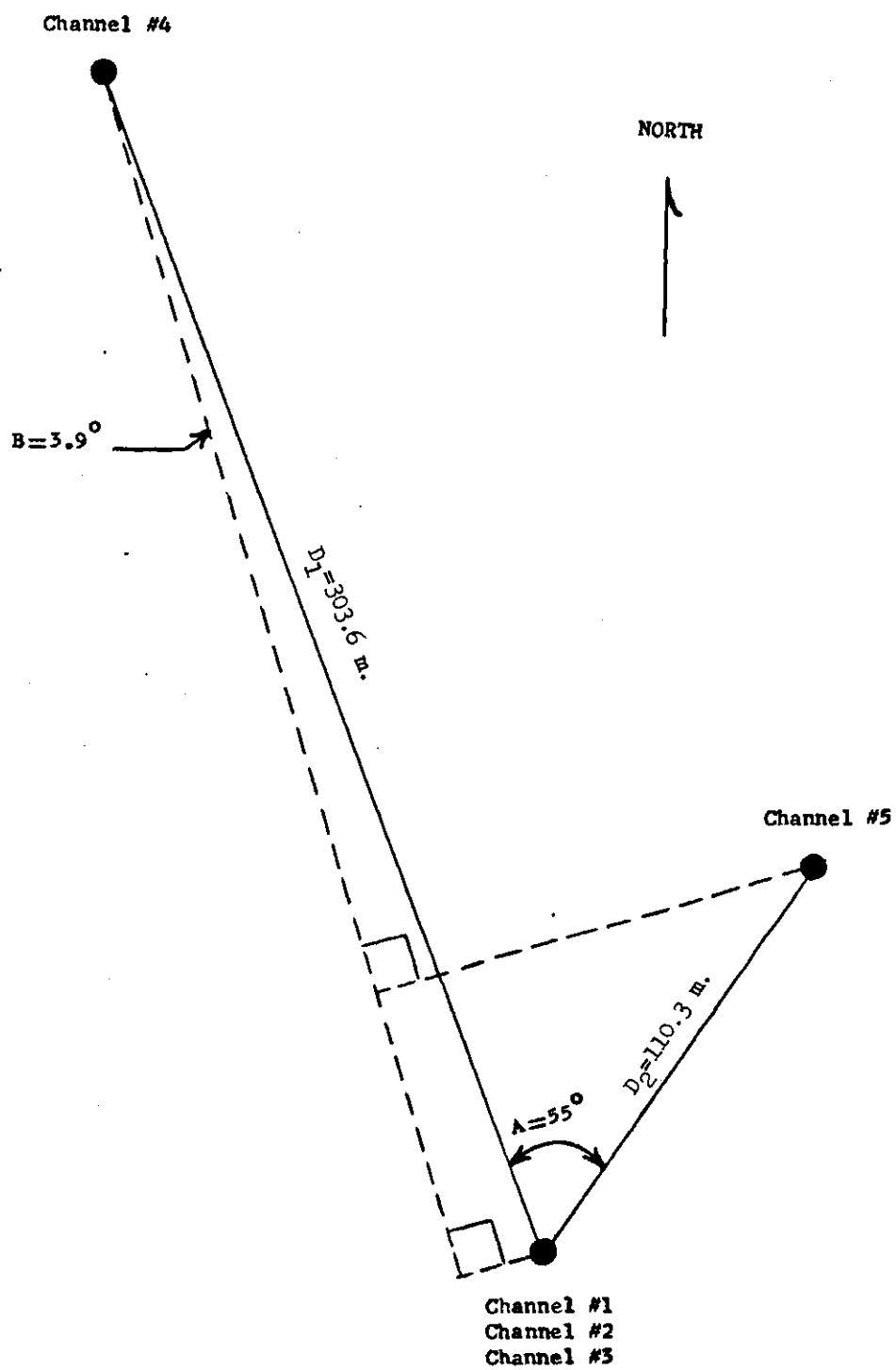


Figure 11. Angles and Dimensions of the Carn Farm Geophone Array.

techniques to equation (2). The errors for ΔV and B were computed as follows:

$$\Delta V = \sqrt{\left(\frac{\partial V_{\text{ap}}}{\partial t_2}\right)^2 \Delta t^2} \quad B = \arccos\left[\frac{(V_{\text{ap}})(t_2)}{D_1}\right]$$

$$\Delta V = 0.7 \text{ km/sec} \quad \Delta AZ = \Delta B = \sqrt{\left(\frac{\partial B}{\partial V_{\text{ap}}}\right)^2 (\Delta V_{\text{ap}})^2 + \left(\frac{\partial B}{\partial t_2}\right)^2 (\Delta t_2)^2}$$

$$\Delta AZ = 2.1^\circ$$

Therefore, the apparent velocity across the array at Carn Farm was $6.3 \text{ km/sec} \pm 0.7 \text{ km/sec}$. Using the refraction lines of Woollard et al. (1957) located nearest Bowman, an approximate value of 0.1° to the southeast was computed as the local dip of the basement. The maximum effect of this dip on the velocity across the array was computed to be $\pm 0.1 \text{ km/sec}$. Therefore, the apparent velocity may be taken as a valid basement velocity.

Measured clockwise from the north, the azimuth (AZ) from the south corner of the array to the seismic source of the 1973 March 22, 14h42m GMT event was $343.5^\circ \pm 2.1^\circ$ (Figure 8).

CHAPTER IV

GRAVITY DATA

Excluding base stations, 344 new gravity readings have been obtained in the vicinity of Bowman, South Carolina. These have been combined with existing data (courtesy of Dr. G. P. Woollard) and contour plotted to produce a regional Bouguer anomaly map (Figure 12). The most distinctive feature of the regional map is a 20 mgal high northeast of the epicentral area which extends into a +12 mgal linear anomaly and runs through the epicentral region and to the southwest. The location of the epicenters of microearthquakes near the linear gravity high contradicts the proposal of Taber (1914) that South Carolina coastal plane earthquakes are the result of movement along existing faults in Triassic basins. In addition, the regional gradients are seen to be much too gentle to represent large faults in the basement. Since the observed gravity highs probably are not caused by variations in the depth to basement, they are most likely the expressions of density contrasts in the basement. The existence of a basement rock of high density which is responsible for the linear gravity anomaly is compatible with the apparent velocity observed at Carn Farm.

The epicentral region is mapped in greater detail in

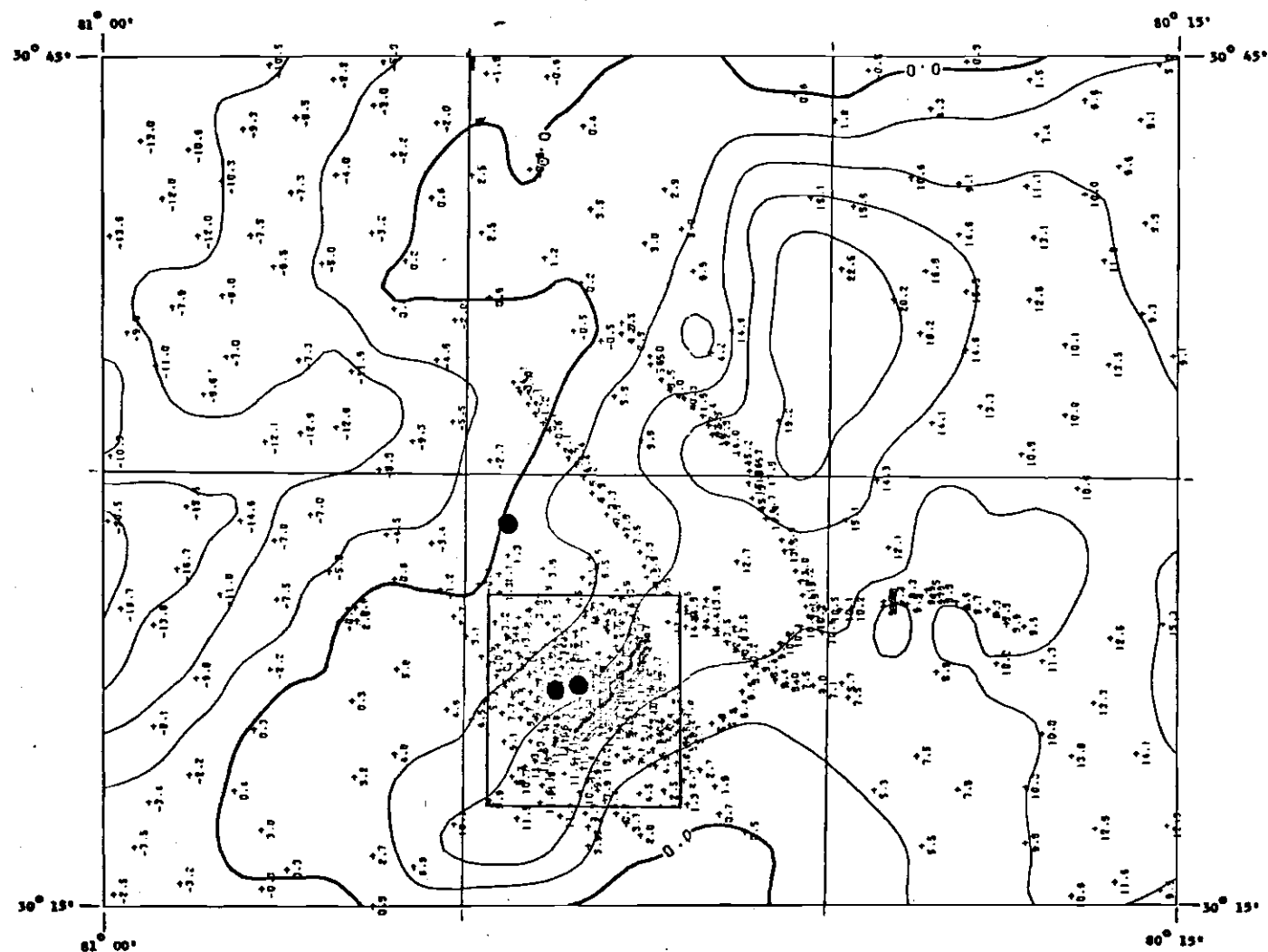


Figure 12. Regional Simple Bouguer Anomaly Map. Epicenters are Indicated and the Area of the Smaller Scale Bouguer Anomaly Map is Outlined.

Figure 13. There are irregularities in the NE-SW trending linear gravity anomaly. Near the epicentral region the width of the anomaly is constricted and its magnitude decreased. Two gravity profiles (Figure 13) perpendicular to the strike of the linear anomaly were used to develop models representative of basement density contrasts which could be responsible for the observed anomaly (Figure 14). A model varying in width from 6 km to 7 km and extending downward for 10 km to 12 km produces a gravity profile the shape of which agrees well with the shape of the profiles along lines 1 and 2. The gravity values of the theoretical profiles closely resemble the observed values along profiles 1 and 2, provided the models, which represent hypothesized structures, are assigned positive density contrasts with the surrounding basement material of 0.1 gm/cc to 0.09 gm/cc. With the exception of Shiloh Church, all of the smoked paper seismograph recording sites were over the modeled structure. This lends support to the 6.9 km/sec basement velocity required to achieve convergence for the epicenter location computed for the 1972 December 16, microearthquake.

The models discussed above can not explain the perturbations observed along the 0 mgal anomaly lines of Figure 12 nor the smaller perturbations observable in the 1 mgal contours of Figure 13. These irregularities (see Profile 2, Figure 13) in the contour lines defining the linear gravity anomaly appear to strike NW-SE, running essentially

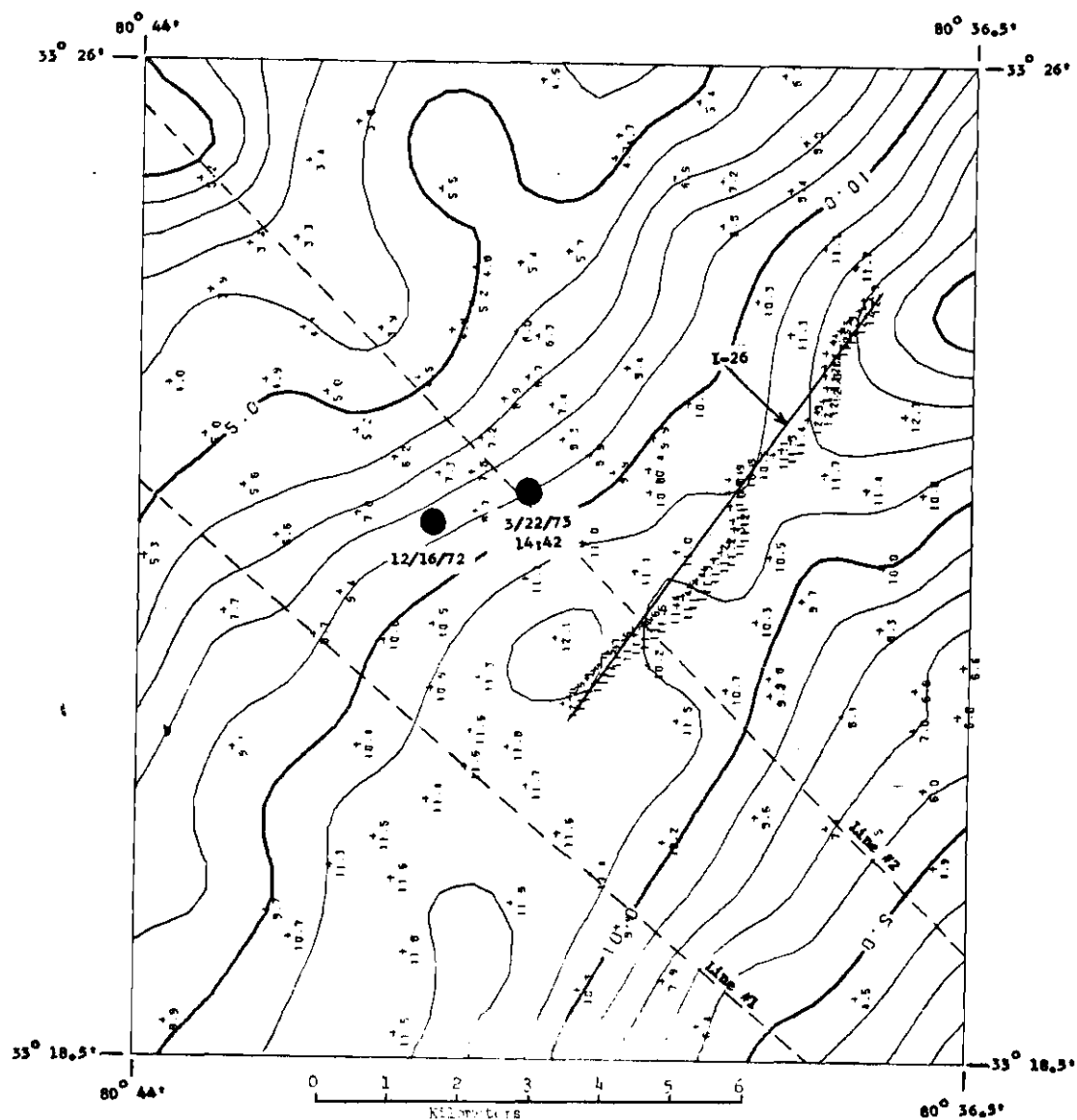


Figure 13. Simple Bouguer Anomaly Map of the Principal Epicentral Area. Epicenters are Located and the Gravity Profiles 1 and 2 are Indicated. Solid Line Along the Axis of the Linear Anomaly is the Line onto which the Detailed Gravity Line Data were Projected to Produce the Profile in Figure 15.

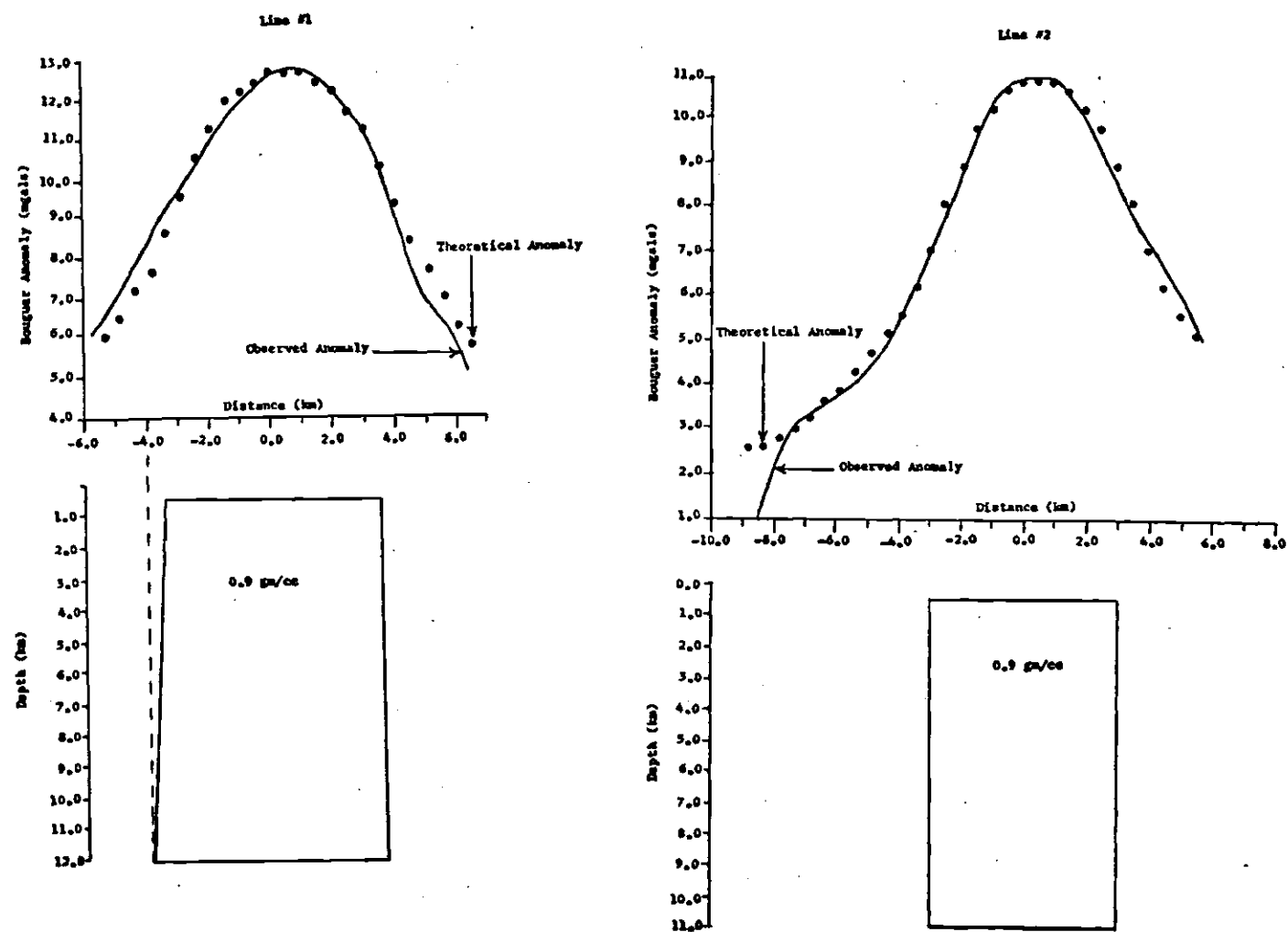


Figure 14. Comparison of the Theoretical Gravity Profiles of Two Basement Structure Models to the Profiles Along Gravity Lines 1 and 2.

perpendicular to the modeled structure and passing very near the epicentral region. The perturbations may reflect changes in thickness of the structure responsible for the linear gravity anomaly or may be the result of a basement feature unrelated to the source of the anomaly.

A line of closely spaced (on the order of 150 meters) gravity readings were made along a portion of the axis of the linear gravity anomaly in an attempt to specifically identify the nature of the NW-SE trending perturbations. The location of the gravity line is delineated by the closely spaced data points in Figure 13. A very sharp 1.3 mgal jump in gravity values occurs along the detailed line near its intersection with interstate 26 (Figure 15). The validity and effect of the Bouguer reduction density was tested by comparing a series of Bouguer gravity profiles of the detailed line with the elevation profile. Each profile in the series was calculated after assuming a different value for the Bouguer density within the range of 2.0 gm/cc to 3.0 gm/cc (Figure 16). The profile which has the least correlation with the sharp irregularities of the topography is preferable (Grant and West, 1965). Since all of the profiles in Figure 16 show equal correlation with the topography, the standard choice of 2.67 gm/cc for the Bouguer reduction density is as appropriate as any other.

If there was a density contrast between the faulted bed and the overlying material, a horizontal bed having a

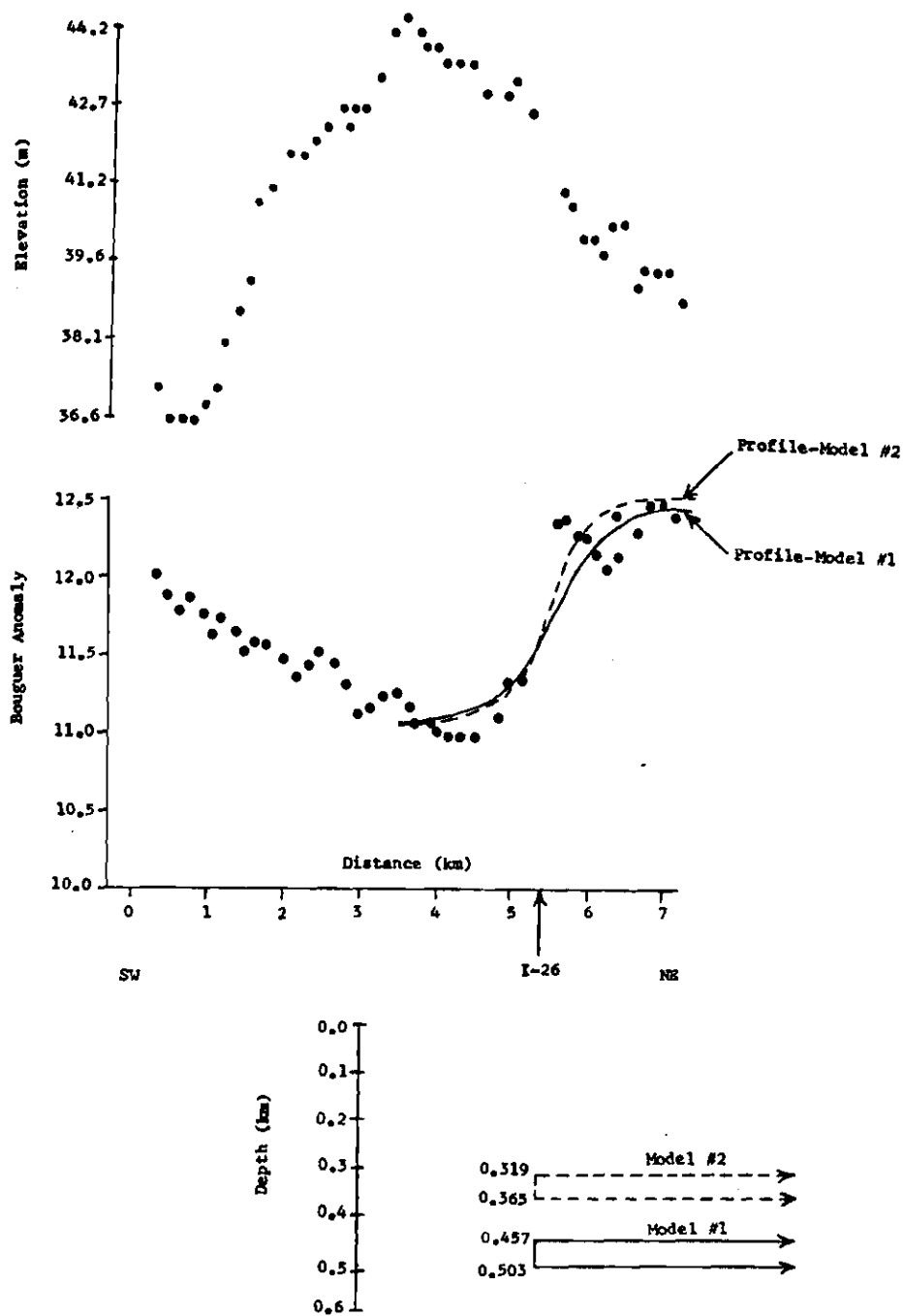


Figure 15. Comparison of the Theoretical Gravity Profile of Two Fault Models to the Steep Anomaly Observed along the Line of Dense Gravity Data.

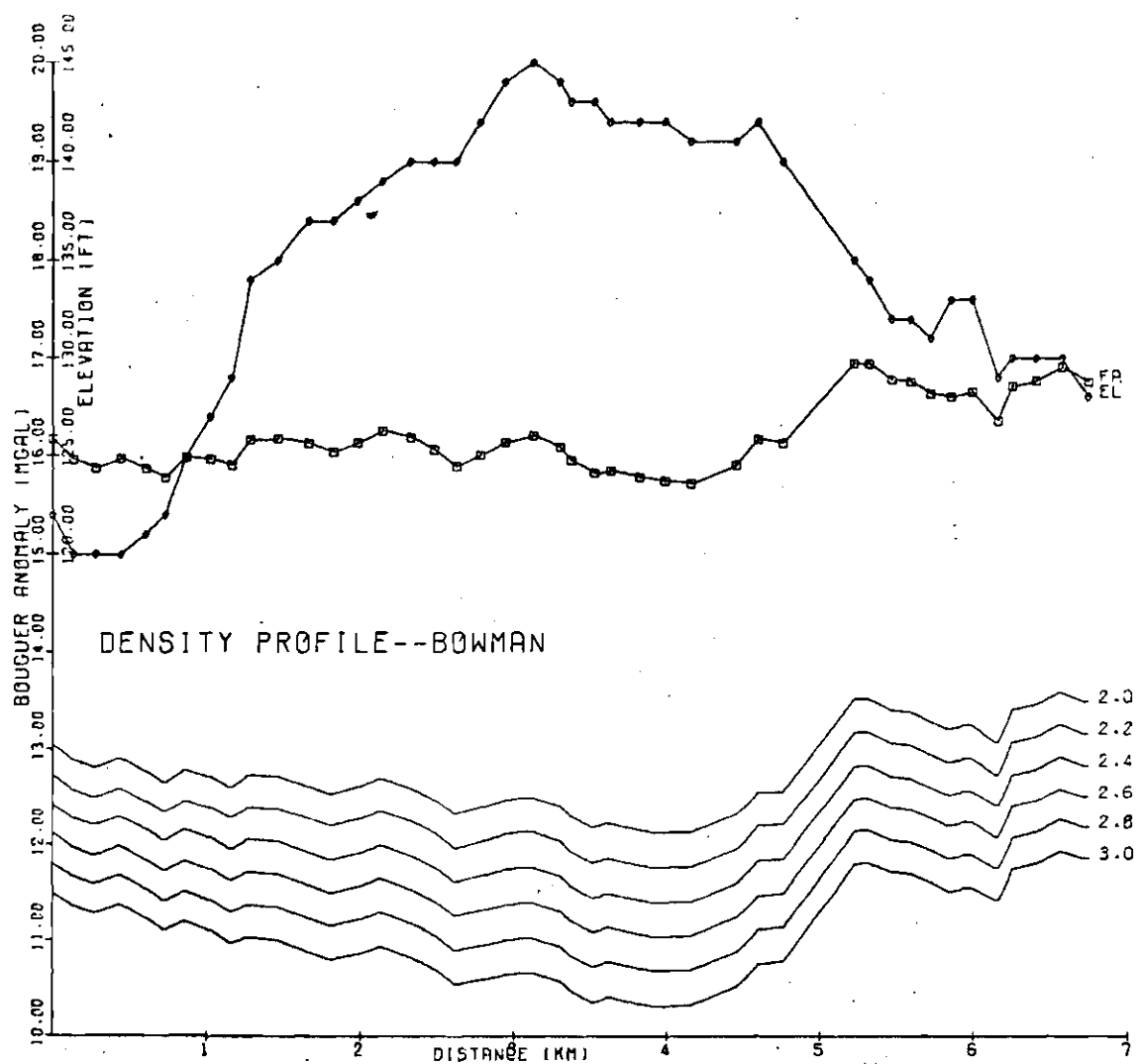


Figure 16. Elevation, Free Air Anomaly, and Plots of the Simple Bouguer Anomaly of the Detailed Line with Different Values for the Bouguer Reduction Density.

normal fault would produce a similar anomaly along a profile perpendicular to the vertical edge of the fault. This situation can be modeled using a semi-infinite horizontal slab of uniform thickness which ends with a vertical edge on one side. The depth to the top of the slab represents the depth to the fault and the density assigned the slab represents the density contrast between the faulted bed and the overlying material.

Using the density-velocity curves of Woollard (1959), a surface layer with a velocity of 2.4 km/sec would have a density of 2.1 gm/cc. Similarly, for a basement rock with a velocity of 6.9 km/sec the density would be 3.0 gm/cc.

The technique of Talwani, Worzel and Landisman (1959) was used to compute the gravity profile of a two dimensional model representing a fault. The density of the slab was taken to be 0.9 gm/cc and the top of the slab was placed at 0.46 km which is the assumed depth to basement in the Bowman area. When the two dimensional model was given a thickness of approximately 46 meters, the amplitude of the gravity profile of the model closely approximated the 1.3 mgal jump observed in the profile of the detailed line. The gravity profile of the model was much smoother than the observed jump. Since the shape of the theoretical profile was dependent only on the depth of the model, the top of the slab was raised above the basement so that the theoretical profile would more nearly match the observed profile. This strongly

suggests that the structure which is responsible for the sharp anomaly in the detailed line extends above the basement into the surface layer material.

A second derivative simple Bouguer anomaly map which includes the first detailed line data exhibits some evidence of a NW-SE trending feature. There is no topographic evidence of the high ridge or of the possible fault line in a second derivative elevation plot of the same area. This is not surprising since the surface geology of the area is such that any elevated features would be subject to rapid weathering and erosion.

If the sharp anomaly of the first detailed line is taken to be the expression of a fault, the continuity of the linear anomaly across the fault plane suggests that there has been less than 2.0 km cumulative horizontal movement along the fault.

CHAPTER V

MAGNETIC DATA

Magnetic data for Bowman and the surrounding area were taken from an aeromagnetic map of the Savannah River Plant area (Petty, et al., 1965). The data (Figure 17), contour plotted with an interval of 100 gammas, show a +2,500 gamma ridge which correlates with the positive ridge shown on the gravity plots and tends to support the possibility that a diabase structure in the basement is responsible for the anomalies. The magnetic data end a few kilometers east of Bowman. The flight lines along which the data were taken run NW-SE, therefore, the data can not directly observe NW-SE trending structures.

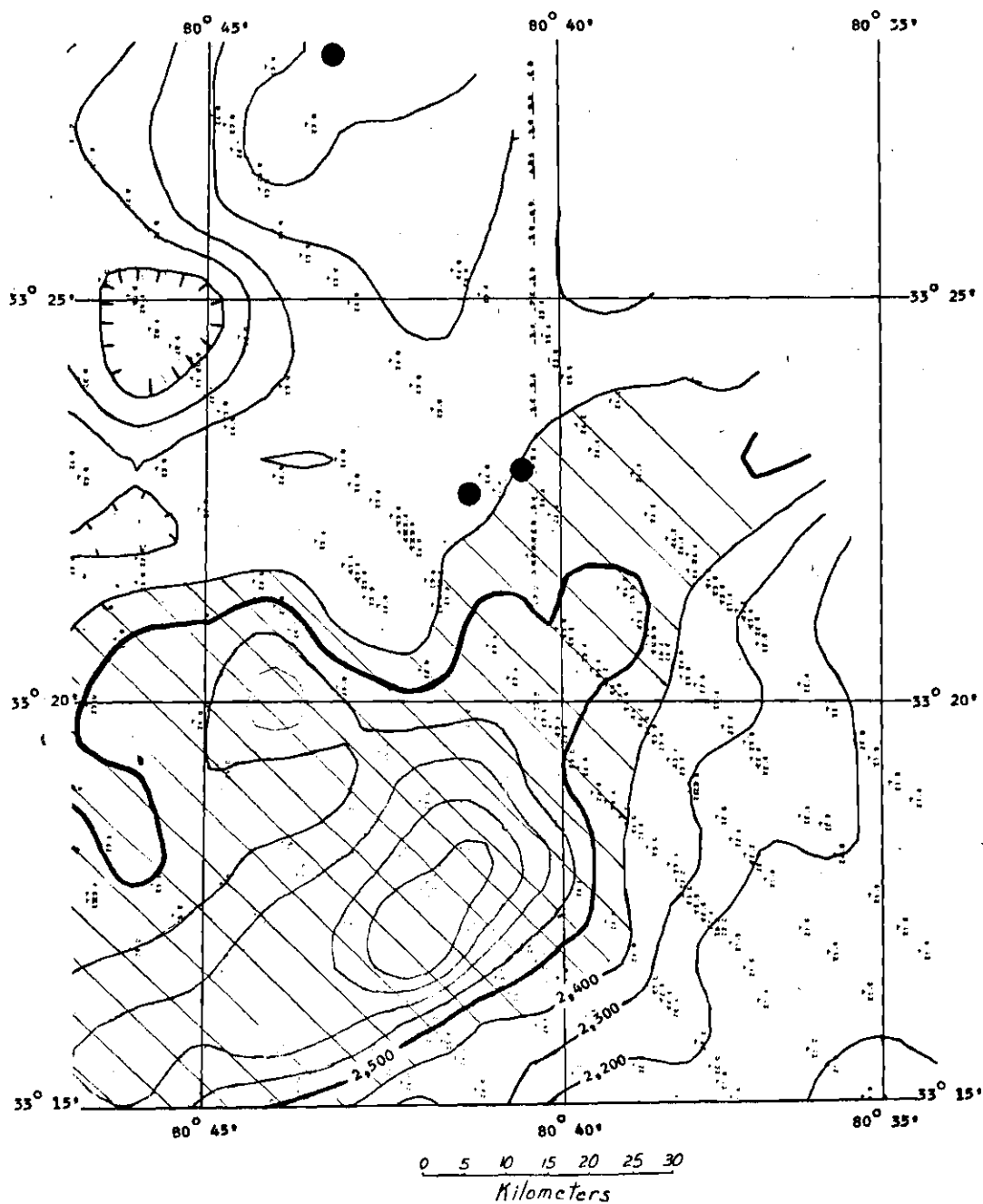


Figure 17. Contour Plot of Aeromagnetic Data Taken from Map of the Savannah River Plant Area. Ridge of Positive Magnetic Values is Crosshatched and Bowman Microearthquake Epicenters are Indicated.

CHAPTER VI

DISCUSSIONS AND CONCLUSIONS

The location of the 1972 February 3, earthquake near Bowman suggests the presence of an active fault and micro-earthquake reconnaissance data shows a continuing sequence of microearthquake activity in the area.

The epicenters of the 1972 December 16, microearthquake and the 1973 March 22, 14h42m GMT microearthquake are very near each other. The location of the 1973 March 22, 06h42m GMT event, however, is approximately 12 km north of the two other epicenters. The (S-P) time of the 1972 August 8, microearthquake indicates that its epicenter does not agree with either of the previously discussed locations. This indicates either that seismic activity is occurring at several points along a single NW-SE trending fault or that more than one fault is responsible for the microearthquake activity near Bowman.

Another indication that the microearthquakes recorded near Bowman may not share a common origin is the difference in character of the seismograms of the various events. The Meyers Farm record of the 1972 August 8, event exhibits a fairly high amplitude refracted P phase. The record of the 1972 December 16, microearthquake which was recorded on the

same site by a similar instrument, shows a very low amplitude refracted P phase. This implies that the events either did not share a common raypath or that their focal mechanisms differ.

Other evidence indicates that the three located events may have occurred at different depths. The refracted P phase of the 1973 March 22, 14h42m GMT event was greater than or equal to the amplitude of the refracted S phase on all records of this event. This characteristic, unique to the records of the 1973 March 22, 14h42m GMT event, may be indicative of a deeper focal depth. Indeed, the epicenter of this event is most precisely located when a depth of focus of 0.61 km is assumed. The two other events are most precisely located when a focal depth of 0.46 km is used in the travel time computations. However, these depths may be no better than order of magnitude estimates of the actual focal depths.

The data obtained during the microearthquake reconnaissance surveys near Bowman are insufficient to locate a fault plane in the vicinity of Bowman. However, recent seismic activity in areas adjacent to Bowman have served to define more clearly the hypothesized NW-SE trending belt of seismic activity that passes through the Bowman area. Two events were reported felt in Lexington, South Carolina on March 7, 1973, at 08:00 GMT and 11:00 GMT. Portable smoked paper seismographs were operating in Bowman at the time but

the ratio of signal to noise was too small to permit a positive identification of these events. Additional micro-earthquakes were recorded by a seven station NOAA seismic array which was operating in the coastal region of South Carolina. Events which were recorded and located by the NOAA array in the period from March to July of 1973, have been plotted in Figure 18 (data courtesy of Art Tarr). Other events which were recorded but which could not be located have been omitted. Figure 18 also shows the location of the Bowman and Lexington events which occurred in the interval from March to July of 1973. Whereas the Columbia-Lexington and Summerville-Charleston areas have histories of seismic activity extending over many years, the Bowman area was apparently seismically inactive prior to the 1971 May 19, event and its successors. The linear alignment and close proximity in time of the events plotted in Figure 18 suggests that the events may be related in some manner. Data are insufficient to conclude that these events occurred along a common fault zone but the possibility warrants investigation by future seismic surveys.

The apparent basement velocity of $6.3 \text{ km/sec} \pm 0.7 \text{ km/sec}$ which was obtained from the Carn Farm array data lends support to the basement velocity of 6.9 km/sec which was used in the epicenter location computations for the Bowman microearthquakes. Velocities in the range from 6.1 km/sec to 6.9 km/sec have been measured in diabase

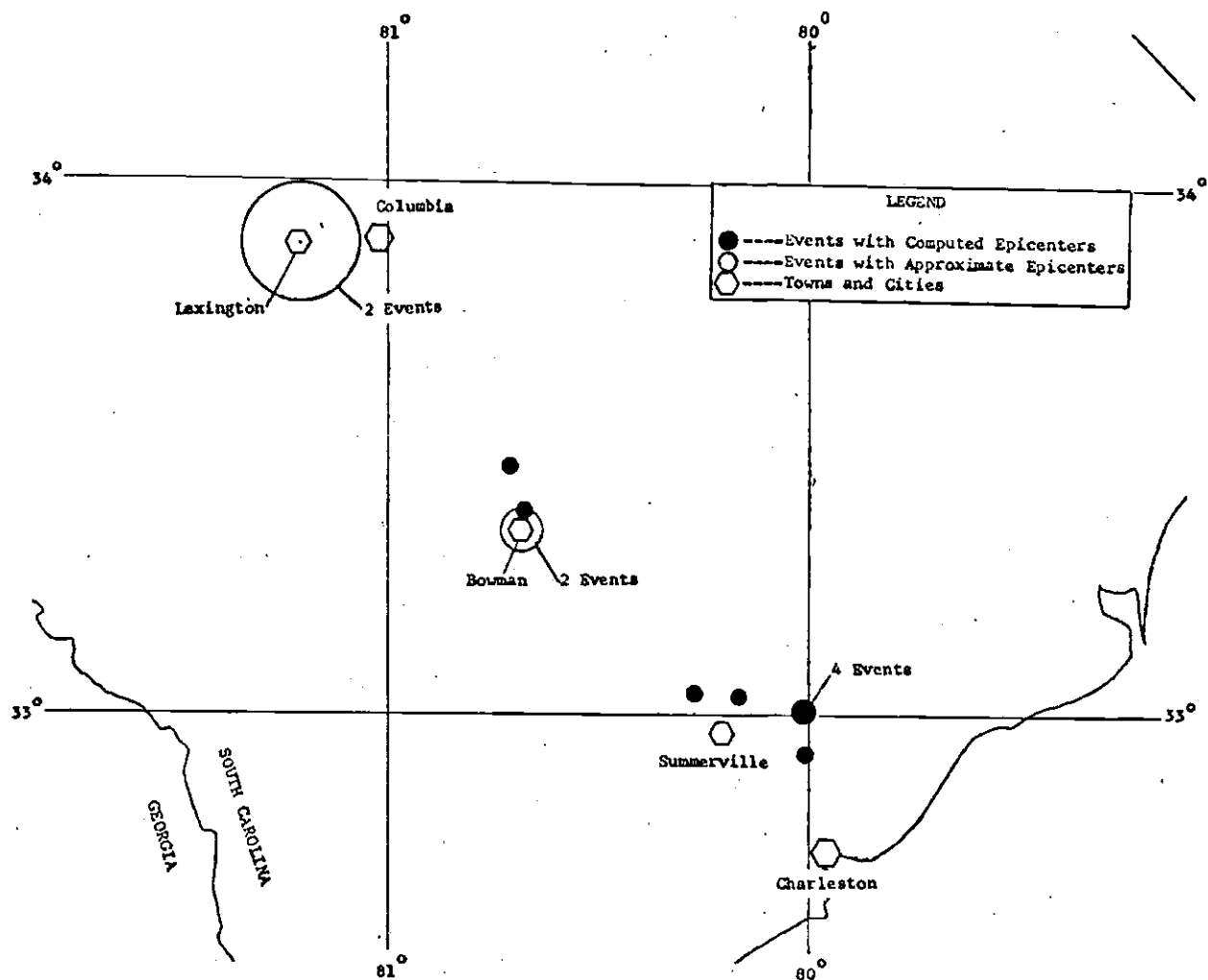


Figure 18. Plot of Bowman and Lexington Events which Occurred from March to July, 1973. Also Included, NOAA Events which Occurred in the Same Time Interval and for which Epicenter Locations were Computed. Size of Open Circles Indicates Uncertainty of Location.

(Anderson and Lieberman, 1966). Seismic refraction work by Pooley (1960) shows that velocities in the range of 6.4 km/sec to 7.0 km/sec have been observed at other locations in the Coastal Plain. Pooley has attributed these high velocities at least in part to the presence of diabase.

The positive linear gravity anomaly suggests that the velocities used in the analysis of the seismic data are appropriate. The linear anomaly that passes through the epicentral region may be the expression of a dense structure at the basement which varies in width from 6 km to 7 km and which extends downward for 10 km to 12 km. Such a structure would explain the high basement velocities that are indicated by the seismic data. The magnetic data which is compatible with the gravity data, also suggests a basement structure composed of material with a greater susceptibility than the surrounding basement material. Diabase appears to be a reasonable material for the basement structure and the presence of such a diabase structure would simultaneously explain both magnetic and gravity anomalies. This possibility will remain unproven until deep well data is obtained for the epicentral region.

The Bouguer profile of the detailed gravity line shows a steep 1.3 mgal jump which can be simulated by a model of a normal fault with a throw of approximately 46 meters. Perturbations in the gravity field of the linear anomaly suggest that the feature responsible for the sharp anomaly in the detailed line strikes NW-SE.

CHAPTER VII

RECOMMENDATIONS

If more microearthquakes were recorded by arrays of seismographs having good time control, the additional seismic data might lead to the successful definition of the fault plane through the Bowman area. Microearthquakes recorded by arrays of sufficient size would also yield much needed focal depth information which would aid in determining the vertical extent of the hypothesized fault. A spectral analysis of the taped records of the 1973 March 22, 14h42m GMT event could possibly yield some information about the focal mechanism of that event. Since events have been reported to the NW and SE of Bowman, it would also be interesting to place portable seismographs between Bowman and these reported events, thus serving to better define the extent and width of the belt of seismic activity which passes through Bowman.

Additional lines of detailed gravity data taken parallel to the first detailed line but displaced to the NW-SE should indicate whether the sharp anomaly is due to an extended feature or to a local perturbation in the subsurface structure. The configuration of the structure could also probably be investigated by carefully executed

refraction lines through the epicentral region and along the axis of the linear anomaly. In addition, high altitude photographs of the Bowman area might serve to locate any faults having surface expression.

APPENDIX I

ANALYSIS OF SEISMIC DATA

The seismic systems used in the microearthquake reconnaissance surveys were Sprengnether portable smoked paper seismographs, two of which were on loan from Virginia Polytechnical Institute, courtesy of Dr. Gilbert Bollinger. Two types of geophones were used with the recorders. When possible, a Hall-Sears HS10-1A 1 Hz geophone was used, but in a few cases an array of 15 Hz exploration geophones was used. Typically, the systems were operated with voltage gains of from 1,000 to 25,000. At 30 Hz, displacement gains generally ranged from 50 k to 100 k at night but these had to be reduced to 25 k to 80 k during the noisier daylight hours. System response curves for the combination 1 Hz geophone and amplifier system and 15 Hz exploration geophone and amplifier system were developed using the technique of Espinose, et al. (1962). The acceleration response curves and particle velocity curves for the systems are plotted in Figure 19.

Smoked paper records of microearthquakes were contact printed on 35 mm film and then enlarged by a factor of 15 with a microfilm printer. This permitted a more accurate measure of (S-P) times than is generally practical from the

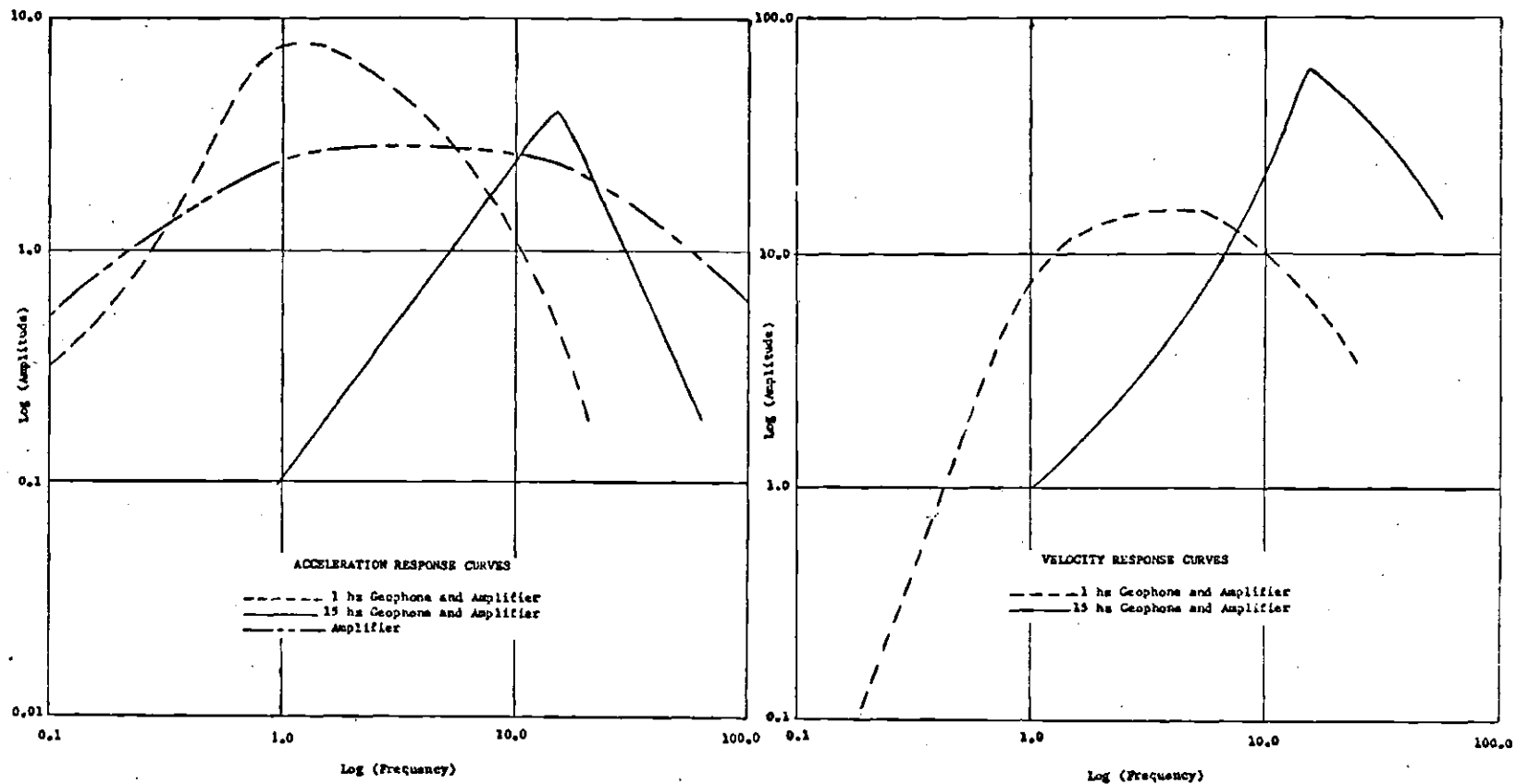


Figure 19. Acceleration Response Curves for the 1 Hz Geophone and Amplifier System, the 15 Hz Geophone and Amplifier System, and the Amplifier. Particle Velocity Curves for the Two Geophone and Amplifier Systems.

original seismograms. For location of the events, standard time-distance relations were used to compute a theoretical (S-P) time for a given epicenter location. This was done for all stations which recorded the event and a total standard deviation was computed based on the deviation of the observed (S-P) time for each recording station. A grid of epicenter locations was projected over the epicentral area and a total standard deviation value was computed for each grid location. Grid intervals of 1 km E-W and 0.3 km N-S were used. The epicenter choice representing the smallest total standard deviation of theoretical (S-P) times from observed (S-P) times could be chosen to a precision of less than one grid interval. Confidence ellipses which were derived from the printed grid values were used to determine the precision of each microearthquake epicenter location. All the computations were performed by a fortran program "Error Grid." The epicenters plotted in Figures 5 and 7 are the locations calculated by the "Error Grid" program. A printout of "Error Grid" is provided in this appendix.

A fortran program "Do-All," which was developed by Dr. L. T. Long to compute the location of Southeastern earthquakes, was modified to provide a check for the "Error-Grid" locations of the Bowman microearthquakes. The program was written to employ the technique of Wiggins (1972) to find an origin time and epicenter corresponding to the least mean squares fit of the observed travel times to theoretical

travel times. The least mean squares technique requires an initial guess with a small error. The location computed by "Error Grid" was used as the first guess for the "Do-All" program. If the location computed by "Do-All" was very near the "Error Grid" location and the adjustment to the origin time computed by "Do-All" was small, this was accepted as a confirmation of the "Error Grid" epicenter location. A printout of the "Do-All" program is included in this appendix.

Printout of the "Error Grid" Program

```

C*****THIS PROGRAM CAUSES THE ERROR SUBROUTINE TO PRINT OUT AN ERROR
C*****MATRIX FOR SEVERAL DIFFERENT POSSIBLE FOCAL DEPTHS. DATA FORMAT
C*****SAME AS FOR DO-ALL.
      DIMENSION DEPTH(3)
      COMMON IPH(20),Q(20),ID(20)
      DAT, DEPTH/0.0, .209, .457/
C*****IPH=PHASE, AZ=FOCAL DEPTH, ID=STATION IDENTIFICATION NUMBER
      N=1
      4 READ(5,102) IPH(N),Q(N),SI,E7,ID(N)
      102 FORMAT(2X,11,2(2X,F7.3),2X,F5.3,2X,I1)
      IF(IPH(N).EQ.0) GO TO 5
      N=N+1
      GO TO 4
      5 CONTINUE
      DO 6 I=1,3
        EZ=DEPTH(I)
      6 CALL ERROR(EZ,N)
      STOP
      END

C*****SUBROUTINE ERROR PRINTS OUT A ERROR GRID FOR EARTHQUAKE EPICENTER
C*****LOCATIONS. GRID APPROXIMATELY TO THE SCALE OF A 15 MIN. QUAD. MAP.
      SUBROUTINE ERROR(EZ,N)
      DIMENSION SLAT(4),SLONG(4),ER(500)
      COMMON IPH(20),Q(20),ID(20)
C*****SLAT AND SLONG ARE THE LATITUDE AND LONGITUDE OF RECORDING STATIONS
      DATA SLAT/33.4083,33.3985,33.3630,33.3350/,SLONG/80.6263,
      C80.7192,80.6890,80.6572/
      I=0
      SDEL=0
      SDELS=0
C*****ELA AND ELO ARE THE TOP LEFT COORDINATES OF THE GRID.
      ELA=33.4333
      ELO=80.7167
C*****XINCA AND XINCO ARE THE GRID INCREMENTS.
      XINCA=0.002417
      XINCO=0.01045
      WRITE(6,91)
      91 FORMAT(1H1,29X,'EARTHQUAKE LOCATION ERROR GRID')
      WRITE(6,92)
      92 FORMAT(72X,'GRID COORDINATES, LONG: 80 43MIN--80 38MIN')
      WRITE(6,93)
      93 FORMAT(41X,'LAT: 33 26MIN--33 19MIN')
      WRITE(6,94) EZ
      94 FORMAT(23X,'DEPTH OF FOCUS=',F6.3)
      DO 1 LA=0.48
      DO 1 LO=0.8
      ELAT=ELA-LA*XINCA
      ELONG=ELO-LO*XINCO
      DO 11 NN=1,N
      II=II(NN)
      A=((ELAT-SLAT(II))*111.11)
      B=((ELONG-SLONG(II))*111.11*0.833)
      D=A**2+B**2
      R=SQRT(D)
      IF(IPH(NN).EQ.5) GO TO 303
C*****EQUATIONS FOR TS AND TP ARE GOOD FOR FOCAL DEPTHS FROM 0 TO .457 KM.
      TP=R*(.146-FZ*0.384+0.349)
      DELP=(NN)-TP
      GO TO 101

```

Printout of "Error Grid" (Concluded)

```

303 TS=R*0.253-EZ*0.664+0.606
    DELS=R(NN)-TS
    SDELP=SDELP+DELP**2
    SDELS=SDELS+DELS**2
101 CONTINUE
304 SUM=(SDELS+SDELP)/N
    SDELP=0
    SDELS=0
    I=I+1
    ER(I)=SQRT(SUM)
    IF(I.EQ.9) GO TO 305
    GO TO 10
305 WRITE(6,90)(ER(I),I=1,9)
    I=0
90  FORMAT(17X,9F6.3)
10  CONTINUE
    RETURN

```

Printout of the "Do-All" Program

```

*****TECHNIQUE TAKEN FROM RALPH A. WIGGINS--THE GENERAL LINEAR INVERSE
*****PROBLEM. REVIEWS OF GEOPHYSICS AND SPACE PHYSICS, FEB. 1972, VOL 10--NO. 1
*****OBJECT IS TO FIND (Y0,ELAT,ELONG,EZ) CORRESPONDING TO LMS FIT OF
*****THE OBSERVED TO THEORETICAL TRAVELTIMES.
      DIMENSION C(5),DC(14),S(14),A(14,4),W(4),UP(4),FDP(4),STAT(4),
      CPHAS(6),LABEL(8)
*****DATA LISTS RECORDING STATIONS AND PHASES.
      DATA STAT/3HWGC,3HSHC,3HROW,3HCFM/
      CPHAS/2HPG,1HP,2HPN,2HSG,1HS,2HSN/
*****DATA READ UNDER STANDARD EARTHQUAKE LIST FORMAT
      READ(5,100) IYR,MO,IDA,IHR,MIN,SEC,ELAT,ELONG,INT,BMAG,
      CIST,IQ,SP,(LABEL(J8),J8=1,8)
100 FORMAT(I4,4I2,F3.1,2F7.4,I2,F2.1,2I1,A4,8A5)
*****FOLLOWING CARD READS SOLUTION WEIGHTS
      READ(5,101) WX,WY,WT,WZ
*****THESE IF STATEMENTS ALLOW INPUT WEIGHTS TO DETERMINE WHETHER THE COMPUTED
*****MATRIX IS 4X4, 3X3, OR 2X2.
      IF(WT,LT,0.0001) GO TO 22
      M=4
      GO TO 23
22 M=3
      IF(WZ,LT,0.0001) M=2
23 CONTINUE
101 FORMAT(2X,4F8.3)
      TO=IHR*3600.+MIN*60.+SEC
      N=0
      WRITE(6,105)MO,IDA,IYR,IHR,MIN,SEC,ELAT,ELONG,(LABEL(J8),J8=1,8)
105 FORMAT(2X,I2,IH/,I2,IH/,I4/,4H H=,I2,2X,I2,2X,F4.1/,6H LAT=,
      C F7.3/,7H LONG=,F7.3/,2X,A4,8A5//)
      WRITE(6,200) WX,WY,WT,WZ
200 FORMAT(/2X,'WX=',F8.3,'WY=',F8.3,'WT=',F8.3,'WZ=',F8.3///)
      WRITE(6,106)
106 FORMAT(5X,'STATION',5X,'PHASE',5X,'ARRIVAL TIME')
*****IPH=PHASE IDENTIFICATION, Q=PHASE TIME, SI=DATA WEIGHT, EZ=DEPTH OF FOCUS,
*****ID=STATION IDENTIFICATION
      6 READ(5,102,END=5) IPH,Q,SI,EZ,ID
102 FORMAT(2X,I1,2(2X,F7.3),2X,F5.3,2X,I1)
      WRITE(6,107) STAT(ID),PHAS(IPH),Q
107 FORMAT(///7X,A3,8X,A2,9X,F7.1/)
      IF(ID,LT,1) GO TO 5
      N=N+1
      CALL ATIME(IPH,TO,ID,ELAT,ELONG,EZ,C)
      DC(N)=Q-C(1)
      A(N,1)=C(3)
      A(N,2)=C(4)
      A(N,3)=C(2)
      A(N,4)=C(5)
      S(N)=1.0/SQRT(SI)
      GO TO 6
5 W(1)=SQRT(WX)
  W(2)=SQRT(WY)
  W(3)=SQRT(WT)
  W(4)=SQRT(WZ)
  CALL MAMAN(A,DC,S,W,N,DP,4)
  DO 14 I6=1,4
14 FDP(I6)=UP(I6)*W(I6)
      TO=TO+FDP(3)
      ELAT=ELAT+FDP(1)/111.11
      ELONG=ELONG+FDP(2)/111.11
      EZ=EZ+FDP(4)
      WRITE(6,108) TO,ELAT,ELONG,EZ
108 FORMAT(1H1,'RESULTS ARE:',2X,'TO=',F8.2,2X,'ELAT=',F9.4,2X,
      C'ELONG=',F9.4,2X,'EZ=',F6.3)
      STOP
      END

```

Printout of "Do-All" (Continued)

```

      SUBROUTINE ATIME(IPH,TO,IO,ELAT,ELONG,EZ,C)
      DIMENSION C(5),SLAT(4),SLONG(4)
C*****DATA IS LATITUDE AND LONGITUDE OF RECORDING STATIONS
      DATA SLAT/33.4083,33.3985,33.3630,33.3350/,SLONG/80.6263,
      80.7092,80.6890,80.6572/
      CALL CXY(ELONG,ELAT,SLAT(IO),SLONG(IO),A,B)
      D=A**2+B**2
      R=SQRT(D)
      IF(IPH.EQ.5) GO TO 303
C*****C(1)=THEORETICAL ARRIVAL TIME OF P PHASE DERIVED FROM TRAVEL TIME CURVES
      C(1)=TO+R*(0.146)-EZ*(0.384)+0.349
      C(2)=1.0
      C(3)=(((ELAT-SLAT(IO))*111.11)*0.146)/R
      C(4)=(((ELONG-SLONG(IO))*111.11)*0.146*0.835)/R
C*****0.835=cos(33.6)---LATITUDE CORRECTION
      C(5)=-0.384
      GO TO 304
C*****C(1)=THEORETICAL ARRIVAL TIME OF S PHASE
303 C(1)=TO+R*(0.255)-EZ*(0.664)+0.606
      C(2)=1.0
      C(3)=(((ELAT-SLAT(IO))*111.11)*0.255)/R
      C(4)=(((ELONG-SLONG(IO))*111.11)*0.255*0.835)/R
      C(5)=-0.664
304 WRITE(6,305) SLAT(IO),SLONG(IO),R
      WRITE(6,301)
305 FORMAT(2X,'STATION LATITUDE=',F7.4,2X,'STATION LONGITUDE=',
      CF7.4,2X,'DIST.=',F5.2)
301 FORMAT(2X,'      C(1)      C(2)      C(3)      C(4)      C(5)')
      WRITE(6,302)(C(IO),IO=1,5)
302 FORMAT(2X,F11.3,4(3X,F8.3))
      RETURN
      END

```

```

      SUBROUTINE CXY(XO,YO,ALAT,ALONG,X,Y)
C***** (XO,YO) IS ORIGIN IN DEGREES(500M)FROM DATA FOR < .1KM ERROR
C***** (ALAT,ALONG) LATITUDE AND LONGITUDE OF DATA POINTS
C*****FROM: RICHTER-ELEN SFIS-USING CLARKE SPHEROID
      DIMENSION B(70), AC(70)
      DATA (B(I),I=30,39)/1.847495,1.847721,1.848073,1.848372,
      1.848673,1.848950,1.849290,1.849605,1.849922,1.850242/
      C(AC(I),I=30,39)/1.856937,1.857033,1.857132,1.857231,1.857331,
      1.857435,1.857538,1.857643,1.857750,1.857858/
      DLAT=ALAT-YO
      DLONG=ALONG-XO
      IA=(YO+ALAT)/2.0
      AA=(AC(IA)+(AC(IA+1)-AC(IA))*((YO+ALAT)/2.0-IA))
      AA=AA*60.0*cos(0.01745329*ALAT)
      X=AA*DLONG
      BB=(B(IA)+(B(IA+1)-B(IA))*((YO+ALAT)/2.0-IA))*60.0
      Y=BB*DLAT
      RETURN
      END

```

```

      SUBROUTINE MINVPT(A,X,NM,MM)
C*****MATRIX INVERSION SUBROUTINE, A IS THE INPUT MATRIX, X IS THE OUTPUT
C*****NM=NN+1
      DIMENSION A(5,5),X(4,4)
      DO 9 I=1,NM
      DO 9 J=1,MM
      A(I,J)=X(I,J)
      DO 16 M=1,NM
      A(I,M)=1.
      DO 10 I=2,NM
      A(I,MM)=0.
      DO 11 J=1,NM
      A(MM,J)=0.0/(1+J)/A(I,1)
      DO 12 I=2,NM
      X=A(I,1)
      DO 12 J=1,MM
      A(1-J,J)=A(I,J+1)-X*A(MM,J)
      DO 16 J=1,NM
      A(MM,J)=A(MM,J)
      RETURN

```

Printout of "Do-All" (Concluded)

```

      SUBROUTINE MAMAT(A,DC,S,W,N,DP,M)
C*****MAMAT PERFORMS MATRIX COMPUTATIONS
      DIMENSION A(14,4),DC(14),S(14),W(4),AN(14,4),ATA(4,4),AVRT(5,5),
      ATDC(4),DP(4)
      DO 7 I=1,N
      DO 7 J=1,M
      7 AN(I,J)=S(1)*A(I,J)*W(J)
      WRITE(6,201)((A(IA,JA),IA=1,N),JA=1,4)
201 FORMAT(1H1,4(1X,F12.2)/)
      DO 8 L=1,4
      DO 8 LL=1,4
      8 ATA(L,LL)=0
      DO 9 I1=1,M
      DO 9 J1=1,M
      DO 9 K1=1,N
      9 ATA(I1,J1)=AN(K1,I1)*AN(K1,J1)+ATA(I1,J1)
      WRITE(6,202)((ATA(IB,JB),IB=1,4),JB=1,4)
202 FORMAT(1X///,(4(1X,F12.2)/))
      I1=M+1
      CALL MINVRT(AVRT,ATA,M,M1)
      WRITE(6,203)((AVRT(IC,JC),IC=1,4),JC=1,4)
203 FORMAT(2X///,(4(1X,F12.2)/))
      DO 10 I2=1,4
      10 ATDC(I2)=0
      DO 11 I3=1,M
      DO 11 K3=1,N
      11 ATDC(I3)=AN(K3,I3)*DC(K3)*S(K3)+ATDC(I3)
      WRITE(6,204)(ATDC(IE),IE=1,4)
204 FORMAT(2X///,(4(1X,F12.2)/))
      DO 12 I4=1,4
      12 DP(I4)=0
      DO 13 I5=1,M
      DO 13 J5=1,M
      13 DP(I5)=AVRT(I5,J5)*ATDC(J5)+DP(I5)
      WRITE(6,205)(DP(IG),IG=1,4)
205 FORMAT(2X///,(4(1X,F12.2)/))
      RETURN
      END

```

APPENDIX II

ANALYSIS OF GRAVITY AND MAGNETIC DATA

The gravity data were taken with a North American Geophysical Company gravity meter model AG-1, number 68. This meter can be read to a precision of approximately ± 0.01 mgals. Traverses were closed at least once every six hours, the drift usually being of the order of 0.05 mgal/hr. The Bowman 15 minute Quadrangle map (USGS) which has 10 ft contour intervals provided the elevation data.

Relative latitude errors between scattered stations were responsible for location errors which were certainly less than ± 0.19 km so that the maximum deviation that can be attributed to such errors is 0.14 mgal. Station elevations obtained from the Bowman Quadrangle map were probably in error by a maximum of ± 2.0 meters so that the maximum gravity deviation due to elevation errors is 0.3 mgal.

Two base stations were used in the gravity surveys. The state base station at Vance was used to establish a base station at Walnut Grove Church. Two gravity meters were used to relate Walnut Grove Church to Vance, South Carolina. This precaution insured a precision of ± 0.02 mgal.

During the Bouguer correction to the gravity, a density of 2.67 gm/cc was assumed. The simple Bouguer

gravity values were plotted and contoured on a Calcomp Plotter by the General Purpose Contouring Program (California Computer Products, Inc., 1968). The contouring program used the eight nearest data points to compute grid values. Grid intervals were chosen commensurate with the density of the gravity data. A listing of the newly acquired gravity data for the Bowman, South Carolina area is included in this appendix.

Theoretical gravity profiles were computed by a program which used the technique of Talwani, Wortzel and Landisman (1959). The program, "GPROF", computed and plotted the theoretical gravity profile of two dimensional models. A printout of "GPROF" is listed in this appendix.

Aeromagnetic data were taken directly from the Geological Survey map of the Savannah River Plant area (Petty et al., 1965). The data were plotted and contoured by the General Purpose Contouring Program in the same way as the gravity data.

Printout of the "GPROF" Program

```

C GRAVITY PROFILING FOR 2-DIMENSIONAL STRUCTURES
C GRAVITY FOR 2-DIMENSIONAL STRUCTURES(AFTER-TALWANI,WORTZEL,LANDISMAN)
C INPUT(2110,3F10,3) CARD NO. ONE
C LL=NO. OF POLYGONS, NXZ=NO. OF GRAVITY VALUES, DX=SEPARATION OF
C GRAVITY VALUES, X0=POSITION OF FIRST GRAVITY VALUE, SCALE=PLOT
C SCALE=FOR DRAW
C IF SCALE=0, PROGRAM CALCULATES SCALE
C IF SCALE=13, NO GRAPH IS DRAWN
C INPUT(FREE FIELD) LL CARDS
C NXZ=NO. OF CORNERS OF POLYGON TAKEN CLOCKWISE, DRHO=DENSITY
C CONTRAST, X(I,J),Z(I,J)=COORDINATES OF CORNERS-JTH CORNER OF ITH
C POLYGON
C REPEAT SEQUENCE FOR ADDITIONAL PROFILES
C BLANK CARD AT END TO TERMINATE CALCULATION
DIMENSION DRHO(50),X(50,20),Z(50,20),NM(50),XA(20),ZZ(20),GAL(500)
25 READ (5,500) LL,NXZ,DX,X0, SCALE
WRITE(6,505) LL,NXZ,DX,X0
503 FORMAT(1H1,28HVERTICAL GRAVITY ANOMALY FOR,15, 9H POLYGONS/2X,
13HTHE,15,16H-GRAVITY VALUES,,F10.4,19H-KM,APART, BEGIN AT,F10.4)
IF(LL) 26,26,27
27 DO 100 I=1,LL
500 FORMAT (2110,3F10,5)
READ(5,501) NXZ,DRHO(I),(X(I,J),Z(I,J),J=1,NXZ)
WRITE(6,502) NXZ,DRHO(I), (X(I,J),Z(I,J),J=1,NXZ)
501 FORMAT( )
502 FORMAT(16H NO OF POINTS = ,I10,22H DENSITY DIFFERENCE = ,(1X,10F10
<.3/))
100 NM(I) = NXZ
DO 101 I=1,LL
NM1 = NM(I)
DO 101 J = 1,NM1
101 X(I,J) = X(I,J) -X0
DO 102 I=1,NXZ
G=0.0
DO 103 J=1,LL
NMJ = NM(J)
DO 104 K = 1,NMJ
XX(K) = X(J,K)
104 ZZ(K)=Z(J,K)
CALL TLLZ(NM(J),XX,ZZ,DRHO(J),GA)
103 G= G+GA
GAL(I) = G
DO 110 M=1,LL
NM1 = NM(M)
DO 110 N = 1, NM1
110 X(N,M) = X(N,M)-DX
102 CONTINUE
WRITE(6,505) (GAL(I),I=1,NXZ)
505 FORMAT(1X//24H GRAVITY ANOMALY IN MGAL/(5F15.8))
ISC=SCALE
IF(ISC.EQ.13) GO TO 25
IF(SCALE) 130,131,130
131 CALL MXSCL(NXZ,GAL,SCALE)
130 CALL DRAW(NXZ,1,GAL,SCALE)
GO TO 25
26 STOP
END

SUBROUTINE DRAW (NTOT, INC, F, SCALE)
C NTOT=TOTAL NUMBER OF POINTS IN F. F IS THE DATA (ONE DIMENSIONAL)
C TO BE PLOTTED, INC IS THE SAMPLE INTERVAL FOR PLOTTING F.
C SCALE IS THE AMPLITUDE OF ONE FULL SCALE DEFLECTION
DIMENSION F(NTOT)
DATA AA1/1H /,AA2/1H*,AA3/1H+
WRITE(6,1011) SCALE,(I,I=9,10), (AA2,M=1,2)
1011 FORMAT(1H1,F14.3,17H-MGALS FULL SCALE/2X,20F5/2X,22A5)
DO 1501 K = 1, NTOT, INC
FK = 50.*F(K)/SCALE
AL = FK/50
AK = FK - K1*50.+50.5
WRITE (6,511) AA2, (AA1,I=1,KK),AA2
511 FORMAT (1X,110A1)
1501 CONTINUE
RETURN

```


Printout of "GPROF" (Concluded)

```

      SUBROUTINE TWL7(K1,XX,ZZ,DRHO,GA)
C   USES METHOD OF TALWANI, WENZEL, AND LANDISMAR (JGR 1959 PP 49-59)
C   TO GIVE GRAVITY ANOMALY AT X=0,Z=0. IN MGAL FOR TWO DIMENSIONED
C   BODY IN VERTICAL PLANE DESCRIBED BY A POLYGON (IN KILOMETERS)
      DIMENSION XX(K1),ZZ(K1)
      PI = 3.141592654
      KK = K1-1
      GA = 0.0
      DO 100 K=1, KK
      K2 = K+1
      IF(XX(K)*ZZ(K2)-XX(K2)*ZZ(K)) 30,100,30
30  IF(XX(K)-XX(K2)) 35,20,35
20  XZ = ((XX(K2)**2 + ZZ(K2)**2)/(XX(K)**2 + ZZ(K)**2))
      DG = 0.5*LOG(XZ)*XX(K)
      GO TO 99
35  IF(ZZ(K)-ZZ(K2)) 235,72,235
72  DG = ZZ(K)*(ATAN2(ZZ(K2),XX(K2))-ATAN2(ZZ(K),XX(K)))
      GO TO 99
235  A = (XX(K2)-XX(K))/(ZZ(K2)-ZZ(K))
      B = (XX(K)*ZZ(K2) - XX(K2)*ZZ(K))/(ZZ(K2)-ZZ(K))
      IF(XX(K)) 200,201,200
201  DG = (B/(1.+A*A))*(.5*LOG((XX(K2)+XX(K)+ZZ(K2)+ZZ(K))/(ZZ(K)*
1  ZZ(K))) - A*(ATAN2(ZZ(K2),XX(K2))-PI/2.))
200  IF(XX(K2)) 31,210,31
210  DG = (B/(1.+A*A))*(.5*LOG((ZZ(K2)*ZZ(K)/(XX(K)*XX(K)+
1  ZZ(K)*ZZ(K))) + A*(ATAN2(ZZ(K),XX(K)) - PI/2.))
31  DG=LOG((XX(K2)+XX(K)+ZZ(K2)+ZZ(K))/(XX(K)*XX(K)+ZZ(K)*ZZ(K)))
      DG=(B/(1.0+A*A))*(0.5*DG-A*(ATAN2(ZZ(K2),XX(K2))-ATAN2(ZZ(K),
1  XX(K))))
99  GA=(13.34) *DRHO*DG + GA
100 CONTINUE
      RETURN
      END

      SUBROUTINE FXSCL(N,A,AMAX)
      DIMENSION A(N)
      AMAX = 0
      DO 26 I = 1,N
      IF (ABS(A(I))-AMAX) 26,26,25
25  AMAX = ABS(A(I))
26  CONTINUE
      RETURN
      END

```

BIBLIOGRAPHY

1. Anderson, Orson L. and Robert C. Liebermann (1966). Sound Velocities in Rocks and Minerals, Willow Run Laboratories, Ann Arbor, Michigan.
2. Bollinger, G. A. (1972). Historical and recent seismic activity in South Carolina, Bull. Seism. Soc. Am. 62, 851-864.
3. California Computer Products Inc. (1968). General Purpose Contouring Program.
4. Dutton, C. E. (1889). The Charleston earthquake of August 31, 1886, U. S. Geol. Surv., Annual Report 1887-88, 209-528.
5. Espinosa, A. F., G. H. Sutton and H. J. Miller, S. J. (1962). A transient technique for seismograph calibration, Bull. Seism. Soc. Am. 52, 767-779.
6. Grant, F. S. and G. F. West (1965). Interpretation Theory in Applied Geophysics, McGraw-Hill Book Company, New York, p 241.
7. Long, L. T. (1972). The South Carolina earthquake of February 3, 1972, Earthquake Notes 43, 13-17.
8. Petty, A. J., F. A. Petrafeso and F. C. Moore, Jr. (1965). Aeromagnetic Map of the Savannah River Plant Area South Carolina and Georgia, U. S. Geol. Surv., Geophysical Investigations Map GP-489.
9. Pooley, Robert N. (1960). Basement configuration and subsurface geology of eastern Georgia and southern South Carolina as determined by seismic-refraction measurements, M.S. Thesis, University of Wisconsin.
10. Pooser, William Kenneth (1965). Arthropoda, Biostratigraphy of Cenozoic Ostracoda from South Carolina, University of Kansas, Article 8.
11. Taber, S. (1914). Seismic activity in the Atlantic Coastal Plain near Charleston, South Carolina, Bull. Seism. Soc. Am. 4, 108-160.

12. Talwani, Manik, J. L. Wortzel and Mark Landisman (1959). Rapid gravity computations for two-dimensional bodies with application to the Mendocino Submarine Fracture Zone, J. Geophys. Res. 64, 49-59.
13. White, J. E. (1965). Seismic Waves Radiation, Transmission, and Attenuation, McGraw-Hill Book Company, New York, p 103.
14. Wiggins, Ralph A. (1972). The general linear inverse problem: Implication of surface waves and free oscillations for earth structure, Rev. Geophys. and Space Phys. 10, 251-285.
15. Woollard, G. P., W. E. Bonini and R. P. Meyer (1957). A Seismic Refraction Study of the Sub-Surface Geology of the Atlantic Coastal Plain and Continental Shelf between Virginia and Florida, Technical Report Contract No. N7onr-28512, Univ. of Wisconsin, Madison, Wisconsin.
16. Woollard, G. P. (1959). Crustal structure from gravity and seismic measurements, J. Geophys. Res. 64, 1521-1544.